

A PHOTOELECTRIC INVESTIGATION OF SURFACE
STATES ON INSULATORS

by

ROBERT NORTON NOYCE

SUBMITTED IN PARTIAL FULFILLMENT OF THE
REQUIREMENTS FOR THE DEGREE OF
DOCTOR OF PHILOSOPHY

at the

MASSACHUSETTS INSTITUTE OF TECHNOLOGY

September, 1953

Signature of Author.
Department of Physics, August 14, 1953

Certified by. Thesis Supervisor

Accepted by.
Chairman, Departmental Committee on Graduate Students

A PHOTOELECTRIC INVESTIGATION OF SURFACE STATES ON INSULATORS

Robert N. Noyce

Submitted to the Department of Physics on August 14,
1953 in partial fulfillment of the requirements for the degree of
Doctor of Philosophy

The photoelectric emission from quartz and magnesium oxide was studied. The photoelectric yield as a function of the incident photon energy was determined where possible as a function of the surface treatment and the temperature. The thermionic work function of powdered magnesium oxide was determined.

The results of this research determine an upper limit on the photoelectric yield of clean quartz of 10^{-9} electrons per quantum at a photon energy of 4.65 ev, and of 10^{-7} electrons per quantum at 5.26 ev. The sensitivity of the apparatus was too poor to determine the spectral distribution of the photoemission. It was shown that depositing a fraction of a monolayer of tungsten on the surface of the quartz increased the photoemission by a factor of 1000, and that the photoelectric yield from the surface was then similar to that from tungsten, although smaller in magnitude. The density of the states thus introduced on the surface was shown to be greater than $10^{13}/\text{ev-cm}^2$. The surface however remained nonconducting, with a surface resistance greater than 10^{17} ohms per square.

The photoelectric yield from magnesium oxide was shown to have a structure with peaks occurring at photon energies of 3.1, 3.6 and 4.6 ev. The emission at low photon energies was shown to decay with time lapsed after flashing the sample to a high temperature. Illumination with 4 ev photons caused an enhancement of the emission at 3.4 ev. At 500°C the photoelectric yield was lower than that at room temperature, but at 800°C the yield was higher than at room temperature. The thermionic work function for two samples was determined to be 3.3 and 3.6 volts.

The structure of the photoelectric yield curve for magnesium oxide indicates that the emission arises from impurities in the bulk, and no indication of emission from surface states was found.

Thesis Supervisor: Wayne B. Nottingham
Title: Professor of Physics

TABLE OF CONTENTS

I	INTRODUCTION	
	A. Existence of Surface States	
	Theoretical Work	1
	Experimental Work	4
	B. Object of this Research	
	Previous Work	6
	Interpretation of Photoemission from Insulators	8
	Materials to be Used	9
II	EXPERIMENTAL APPARATUS	
	A. Current Detection	10
	B. Ultraviolet Sources	11
	C. Monochromator	13
	D. Intensity Measurements	13
	E. Vacuum Techniques	17
III	EXPERIMENTS ON QUARTZ	
	A. Samples	20
	B. Tube Construction	22
	C. Tube Assembly and Processing	25
	D. Experimental Procedure	26
	E. Summary of Results	37
IV	EXPERIMENTS ON MAGNESIUM OXIDE	
	A. Samples	38
	B. Single Crystal Magnesium Oxide	38

C. Powdered Magnesium Oxide	
Tube No. 1	43
Tube No. 2	47
Tube No. 3	52
Tube No. 4	54
D. Summary of Results	65
V DISCUSSION OF RESULTS	
A. Results on Quartz	66
B. Results on Magnesium Oxide	68
C. Photoemission for Study of Surface States	73
APPENDIX	74
ACKNOWLEDGEMENTS	76
BIBLIOGRAPHY	77
BIOGRAPHICAL NOTE	79

TABLE OF FIGURES

1. Calibration of Quartz Prism	14
2. Calibration of Calcium Fluoride Prism	15
3. Dispersion of Quartz Prism	16
4. Calibration of 935 Phototube	18
5. Experimental Tube for Study of Photoemission From Quartz	23
6. Charging-Discharging Curves for Tube No. 5	29
7. Photoelectric Yield: Tube No. 5	31
8. Photoelectric Yield after Depositing 0.1 Monolayer Of Tungsten	34
9. Charging-Discharging Curves for MgO	40
10. Experimental Tube for Study of Photoemission From Powdered MgO	45
11. Photoemission from MgO after Various Annealing Temperatures: Tube No. 2	49
12. Photoemission from MgO at High Temperature: Tube No. 2	51
13. Dependence of Thermionic Current on Anode Voltage: Tube No. 3	53
14. Richardson Plot for MgO: Tube No. 3	55
15. Calibration of Platinum Ribbon	56
16. Pressure Variation During Breakdown of $MgCO_3$	57
17. Photoemission from MgO after Various Annealing Temperatures: Tube No. 4	59
18. Decay of Photoemission at Low Photon Energies: Tube No. 4	60
19. Photoemission from MgO at High Temperature: Tube No. 4	61
20. Richardson Plot for MgO: Tube No. 4	62
21. Decay of Photoemission upon Illumination: Tube No. 4	64
22. Optical Absorption of MgO after Weber	69

I INTRODUCTION

A. Existence of Surface States

In the past twenty years the bulk properties of solids have been the object of a number of researches, both experimental and theoretical. Since the advent of the quantum mechanical solution of the periodic potential problem, concepts have been developed which have been confirmed to a large extent by the intense work on semiconductors in recent years. This work has served to indicate that the presence of the surface may well influence these bulk properties. The effect of the termination of the periodic potential at the surface on the electronic structure of the solid has been discussed theoretically by several workers. However, the experimental data are far from exhaustive, and not yet good enough to serve as a guide to theoretical workers.

In studying the periodic potential problem, the boundary conditions are usually simplified by solving for wave functions in an infinite crystal. This simplification obscures the features of interest associated with the surface of the crystal. Tamm⁽¹⁾ was the first to consider the wave functions for a semi-infinite "Kronig and Penny"⁽²⁾ model. He found it possible to have

energy levels with energies lying in the forbidden band, whose wave functions are localized at the surface of the crystal. In this treatment of the semi-infinite crystal, he found one surface state associated with each gap between allowed energy bands in the interior of the crystal, for the one dimensional model used.

Subsequently, surface states were found by Rijanow ⁽³⁾ while considering the wave functions of a thin metallic strip, and using a potential which was periodic within the strip and rose to a higher value at the edges of the end cells.

Maue ⁽⁴⁾ investigated the problem with a potential which was periodic up to the surface $x = 0$, and constant for $x > 0$. Maue's results showed surface states to exist for the nearly free electron approximation, but not for the tight binding approximation.

Goodwin ⁽⁵⁾ next investigated the field of the surface states. By an extension of Maue's method, i.e. a Fourier expansion of the lattice field and the nearly free electron approximation, he was able to get explicit formulae for the wave functions and energies of the surface states in terms of the constants of the crystal field. He showed that surface states exist with propagation vectors in the plane of the surface, and consequently with a spread of energies. In another paper ⁽⁶⁾ Goodwin discussed the tight binding approximation. Due to the difficulty of the general problem, he considered the one-dimensional case of a linear finite chain of atoms, and was able to obtain formulae for the energies and wave functions of surface states in terms of the overlap integrals of the atomic wave functions. He showed that surface states exist if the coulomb

interaction exceeds the exchange interaction, which indicates that Maue's results are not generally applicable for the case of tight binding.

Shockley ⁽⁷⁾ correlated these articles, and showed conditions under which surface states exist in the two cases. He discussed the energy levels for a finite linear chain of atoms as a function of the internuclear distance by a method similar to Slater's ⁽⁸⁾. The nearly free electron approximation and the tight binding approximation correspond to crossed and uncrossed bands in this treatment. For the case of uncrossed bands, surface states exist for the potentials which include the edge effects on the end cells, but not for those in which the end effects are neglected. These surface states have energies lying close to the edge of the band from which they arise. In the case of crossed bands, surface states are found in pairs at approximately the middle of the forbidden band, one arising from the higher allowed band and one from the lower. Shockley points out that the causes for the existence of surface states are essentially different in these two cases, so there is the possibility of two distinct types of intrinsic surface states. He also points out the possibility for electrons to be trapped on the surface by polarization forces with a resulting distortion of the lattice. The models used here have not considered this possibility since the nuclei are equally spaced. In suggesting the extension of these results to three dimensions, Shockley proposes one surface state for each surface atom ($\sim 10^{15} / \text{cm}^2$)

James ⁽⁹⁾ gives a more graphic description of how these

surface states arise. He shows the possibility of matching the slope-to-value ratio of one of the damped wave functions in the forbidden band of the crystal to the slope-to-value ratio of the damped wave function outside the crystal with the corresponding negative energy. This leads to an allowed solution for a state with energy lying in the forbidden band, and wave function localized at the surface.

In addition to the intrinsic surface states discussed above, there is the possibility that electronic states may be introduced in the forbidden band of energies by the adsorption of foreign atoms on the surface. Indeed, there is reason to believe that the adsorption of foreign atoms on the surface may be activated by the existence of intrinsic surface states as discussed by Pollard ⁽¹⁰⁾ so that a clean surface would be difficult to obtain, and intrinsic surface states difficult to observe.

It is also possible that the distortion of the lattice at the surface, or the adsorption of foreign atoms on the surface would alter the energies of surface states as discussed above so that they lie in the allowed energy bands, and consequently could not be distinguished as surface states.

Whether surface states exist in densities high enough to be detected experimentally has never been determined clearly. In the older theories of the rectification at a metal-semiconductor contact, ^(11, 12) the contact potential difference between the metal and the semiconductor was assumed to determine the barrier height, and consequently the depth of the space charge region when the metal and semiconductor were brought together. Experimental verification

of this hypothesis was uncertain. Meyerhoff⁽¹³⁾ measured the contact potential difference between silicon and various metals, by the Kelvin method, as well as the zero voltage resistance across the contacts between these metals and silicon. He found no correlation between the results. Bardeen⁽¹⁴⁾ explained these results in terms of surface states: i. e. if the density of surface states is high, the dipole layer equal to the contact potential difference will be made up by a change in the population of the surface states, and the barrier height will not be dependent on the metal used to make the contact. He shows that a surface state density of $10^{12} / \text{cm}^2$ would make the barrier height dependent on the metal used for the contact, and a density of $10^{13} / \text{cm}^2$ would very nearly obscure this dependence. Bardeen quotes the results of some workers which show that dependence of the barrier height on the metal used is found for some cases when the metal is evaporated in vacuum, indicating a smaller density of surface states under these conditions. Brattain⁽¹⁵⁾ and Brattain and Shockley⁽¹⁶⁾ have given other evidence for the existence of surface states from experiments on the change of contact potential of silicon upon illumination and upon exposing the surface to various gases. These experiments were not carried out under vacuum, and the authors do not attribute the observed results to intrinsic surface states.

Another piece of evidence which indicates that surface states do not exist to the extent of one per surface atom is the observed surface conductivity of semiconductors and insulators. This is much lower than would be expected if the surface had a half filled continuum of states, as indicated by Shockley.

Thus the density of surface states as estimated from experimental work has been much less than that predicted by the theoretical work which has been done, casting doubt on the whole picture of surface states as they have been derived theoretically.

Apker, Taft, and Dickey⁽¹⁷⁾ discuss the possibility of photoemission from surface states in connection with their work on the photoemission from semiconductors. From the formula⁽¹⁸⁾

$$\sigma = (\pi h/mc)(e^2/h\Delta\nu)F$$

where σ is the cross section for absorption in the range $\Delta\nu$, and F is the oscillator strength, they estimate the absorption cross section of surface states to be $2 \times 10^{-17} \text{ cm}^2$. If there is one surface state per surface atom, and if ten percent of the excited electrons escape, quantum yields of .002 electrons per quantum should be observed. If these estimates are of the right order of magnitude, photoemission from surface states, if not obscured by other effects, should be detectable for densities as low as $10^{11}/\text{cm}^2$, using standard equipment.

B. Object of this Research

Very little work has been done on photoemission from non-metallic compounds. Hughes and Dubridge⁽¹⁹⁾ quote the results of a number of early researches on photoemission from such substances as oxides, sulfides, and other non-conductors. This work was performed some time ago, and nothing more than photoelectric thresholds was determined, the quantum yields being too small for the determination of the associated spectral distributions.

Recently, several workers have measured the spectral

distribution of the photoelectric yield from barium oxide. (20, 21, 22) A steep rise in the quantum yield was noted at 5 ev. Below this energy the emission was variable, and depended on the past history of the sample, and in particular on the method used to prepare the sample. The steep rise at 5 ev. coincides with the edge of the optical absorption band, and is attributed to exciton enhanced emission. The variable emission at lower energies is attributed to variable impurity content in the bulk and on the surface.

Taft and Apker⁽²³⁾ have made a study of the photoemission from rubidium iodide. The yield in this case rises slowly from 2.3 ev to 5 ev, much as the yield for a metal. At 5 ev there is a peak in the yield curve, with the yield decreasing at higher energies. This peak also coincides with the edge of the optical absorption band, and is attributed to exciton enhanced or induced emission. (24) Emission at lower energies is explained as arising from F-centers in the crystal.

Several different interpretations of photoemission from insulating crystals at photon energies less than the band-to-band transition are possible. If the electron affinity of the crystal is negative, photoemission from the valence band would be possible at these photon energies. If the electron affinity is positive, as is usually the case, this would not be possible. Emission from the conduction band will be small since the population of the states is very small. For this case, photoemission at energies less than the band transition must be explained in terms of another mechanism. One possibility is the photoemission directly from impurity levels lying in the

forbidden band. Another is the double mechanism of excitation of electrons into the conduction band from impurity levels and subsequent emission from the conduction band, the necessary energy being supplied either by the incident radiation or the recombination of other electrons or holes with traps. Exciton enhanced emission cited previously is of a similar type. In this case the initial photon produces an exciton (a neutral hole-electron pair) which itself may absorb a second photon resulting in the emission of the electron. A third possibility is the existence of surface states with energies such that emission is possible for photon energies less than the band transition.

If substances could be found in which the last mechanism is the predominant one, photoemission would be a direct method for the study of surface states, and could furnish direct evidence as to their existence. In substances in which the energy gap is small, photoemission from surface states, if occurring, will be masked by emission from the valence band at energies just above the threshold for emission from the surface states. In the work of Apker et al (op. cit.) on semiconductors, photoemission did not occur at energies below that of the band-to-band transition, because of the high work function. Consequently under illumination with photons capable of ejecting electrons, appreciable numbers of electrons are excited into the conduction band as well, again masking effects of surface states. In the case of barium oxide, it has been shown by several workers that a monolayer, or a fraction of a monolayer of free barium is probably adsorbed on the surface, (25, 26) and consequently it is likely that the observed emission is related to these surface

impurities, particularly in view of the result that thresholds for emission from barium oxide and metallic barium are nearly the same.

The object of this research therefore was a study of photoemission from substances for which it was felt that surface states might be the predominant mechanism. The materials studied should, therefore, meet the following conditions as nearly as possible:

They should have a forbidden band wide enough that photoemission from the valence band and exciton generation will not occur at energies comparable with those necessary to remove electrons from surface levels.

They should be free from surface contaminants if intrinsic surface states are to be studied, or should have a controlled amount of a known impurity of the surface if extrinsic surface states are to be studied.

They should be quite pure so that the photoemission from impurity levels, or photoconduction and subsequent photoemission will be small.

The material must be able to withstand adequate outgassing procedures.

Consideration of these factors led to the choice of single crystal and fused quartz, and single crystal and powdered magnesium oxide.

II EXPERIMENTAL APPARATUS

A. Current Detection

Since the light intensities that are available from a monochromator are small, and the quantum yield of photoemission is not large, the currents which must be measured in this type of experiment are extremely small (of the order of 10^{-16} - 10^{-13} amperes.) For that reason electrometer techniques must be used throughout for current measurement. A Compton electrometer was used for the current measurement in the early part of this work. The standard electrometer measurement circuit was employed, the electrometer being used as a null instrument to measure the voltage drop across a calibrated high resistance (10^6 to 10^{12} ohms) caused by the photo-current. For the greater part of the work, however, current measurement was made with a vibrating reed electrometer.⁺ This instrument has several advantages over the Compton electrometer. The noise level of the instrument is .03 mv., and the zero drift rate is less than 1 mv/hour. Such performance figures are hard to achieve with the

⁺ Model 30S Applied Physics Corporation, Pasadena, California

Compton electrometer. The primary advantages of the vibrating reed instrument are the fast time constant, and the fact that the voltage output may be displayed on a recording potentiometer, so that a continuous record may be kept of the current as a function of time. This was a great help in the study of polarization phenomena and transient currents, which would have been unobservable using the Compton electrometer.

The extremely small currents which were to be measured made necessary the shielding of the measurement electrode from stray fields. This was achieved partly by appropriate construction of the tubes and partly by external shielding. The leads to the electrometer had to be carefully insulated and shielded. After trouble was encountered with polystyrene as an insulator for the coaxial lead from the tube to the electrometer, a new arrangement was used that required no insulators other than the glass press of the experimental tube, and the insulator associated with input terminal of the electrometer. Even so, after changing the positions of the tube or the electrometer, it was often necessary to wait for several hours before the background currents fell below 10^{-16} amperes.

B. Ultraviolet Sources

The thresholds of the materials studied were high enough so that most of the work was done in the ultraviolet region of the spectrum. Brilliant sources for this region are few, and three sources were tried during the course of the experiments. A high pressure xenon arc⁺ similar to the 125 watt arc described by Baum and Dunkleman⁽²⁷⁾

⁺ Obtained from Hanovia Chemical Corporation, Newark, N. J.

was used initially. This source provides a high intensity continuum in the ultraviolet. Though of higher intensity than the standard high pressure mercury arcs, such as the H-4⁺ or H-5⁺ lamps, it is essentially a point source. Using the standard input optics the image of the source does not fill the entrance slit of the monochromator, and for this reason was abandoned in favor of the CH-3⁺mercury arc. This lamp, although smaller and operating at less power input than the H-4 or H-5 lamps, runs at higher pressure and is more intense. Its spectrum consists of the characteristic lines of mercury superimposed upon a continuous background. The peaks in the spectrum provided 2 to 5 times the intensity available using the xenon arc, although a continuous background is less intense.

As the research progressed, it became evident that a more intense source would be desirable, since the resulting photocurrents were still small and the current sensitivity had been increased to the limit of the instrumentation. An AH-6⁺ high pressure mercury arc was obtained with its associated controlling equipment for the latter part of the research. This lamp operates at 1000 watts, and has a light output about ten times that of the CH-3. This gave usable light output of about 2×10^{-7} watts at 2500 angstroms, with 1 mm slits in the monochromator, i.e. 18 Å bandwidth at this wavelength.

+ General Electric Company

C. Monochromator

The monochromator used was the Perkin-Elmer Model 83 Universal Monochromator.[†] The monochromator was calibrated using the lines of a low pressure mercury arc as a standard. The calibration of the quartz and calcium fluoride prisms used with the instrument are given in Figs. 1 and 2. The zero setting of the drum scale is arbitrary, and may be changed by means of a set screw on the Littrow mirror mount. After changing prisms, by suitable adjustment of this screw with the monochromator set on one line, the calibration of the prism may be reproduced. The dispersion of the monochromator is plotted in Fig. 3 in terms of angstroms bandwidth per millimeter slit width, and energy bandwidth per millimeter slit width. Front surface mirrors are used throughout the system, so the optics may be used at all wavelengths, and once set will remain in focus.

D. Intensity Measurements

In order to measure the photoelectric yield in terms of electrons per incident quantum, it is necessary to have an absolute calibration of the detector used to measure the incident radiation. The detector employed was an RCA 935 phototube which had been

[†] The Perkin-Elmer Corporation, Norwalk, Conn.

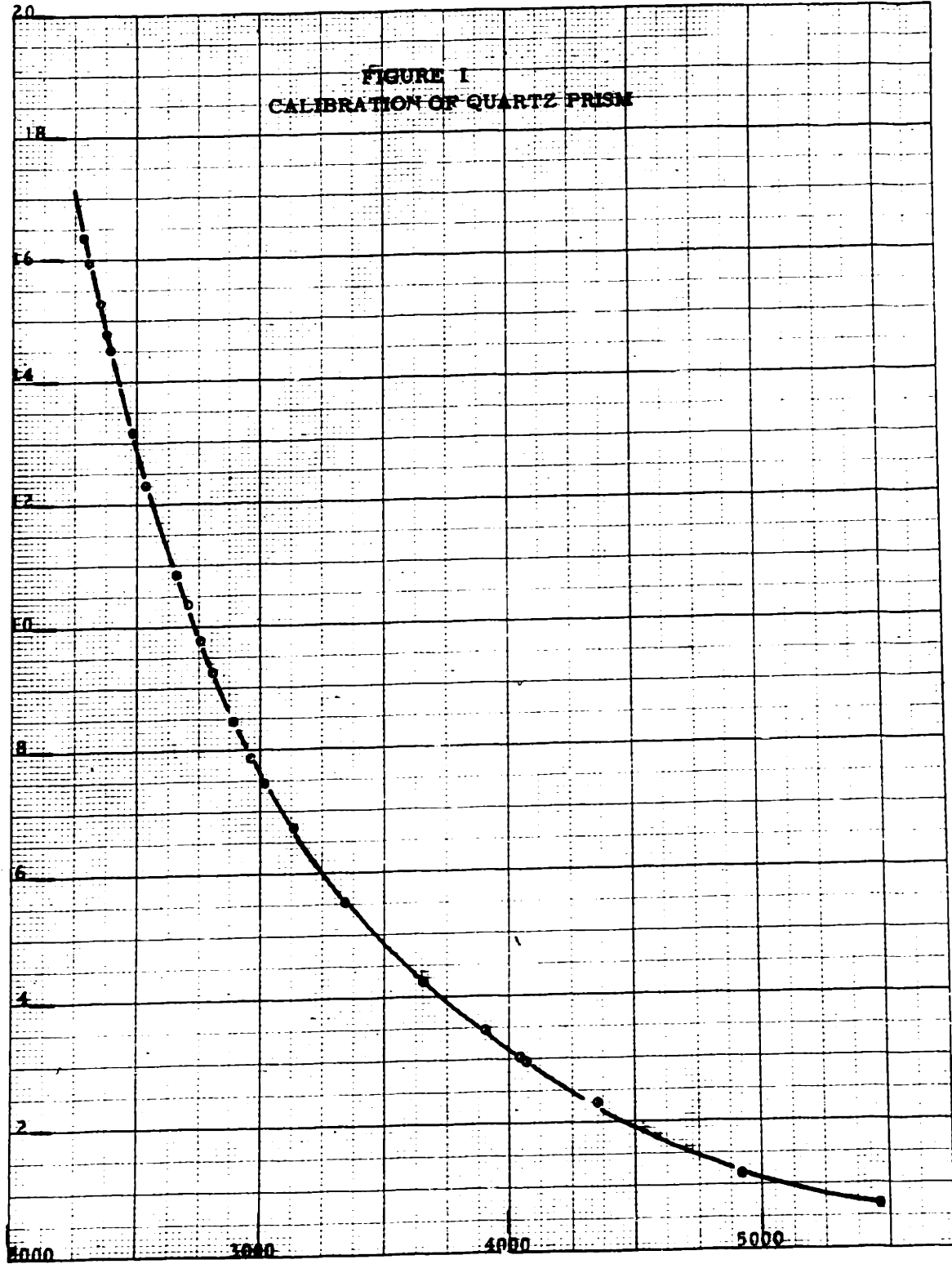
FIGURE I
CALIBRATION OF QUARTZ PRISM

COOPER BROS COMPANY, INC. NORWOOD, MASSACHUSETTS
PRINTED IN U.S.A.



NO. 318A. 20 DIVISIONS PER INCH BOTH WAYS. 180 BY 240 DIVISIONS.

Wavelength Drum Reading



Wavelength Angstroms

FIGURE 2
CALIBRATION OF CALCIUM FLUORIDE PRISM

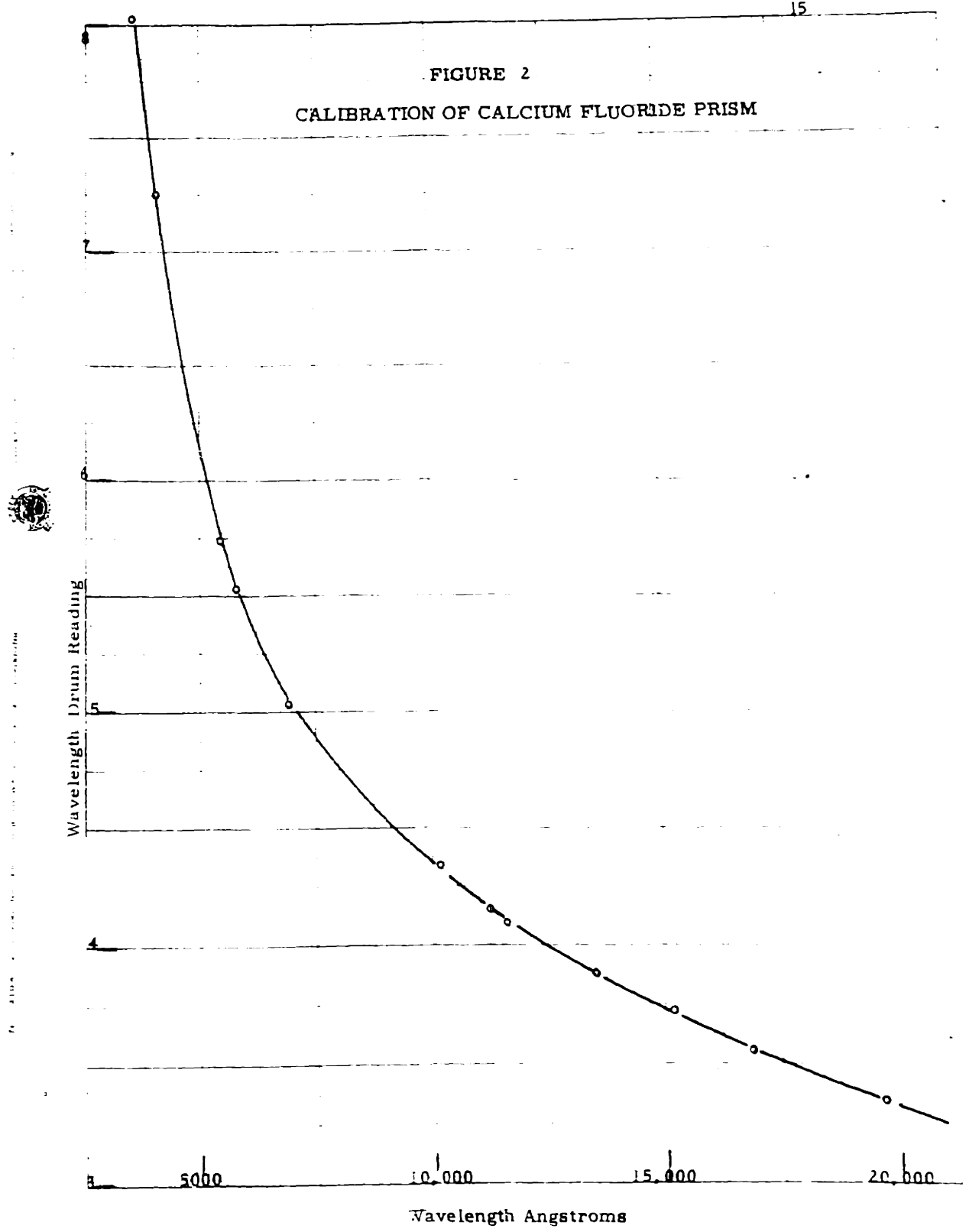
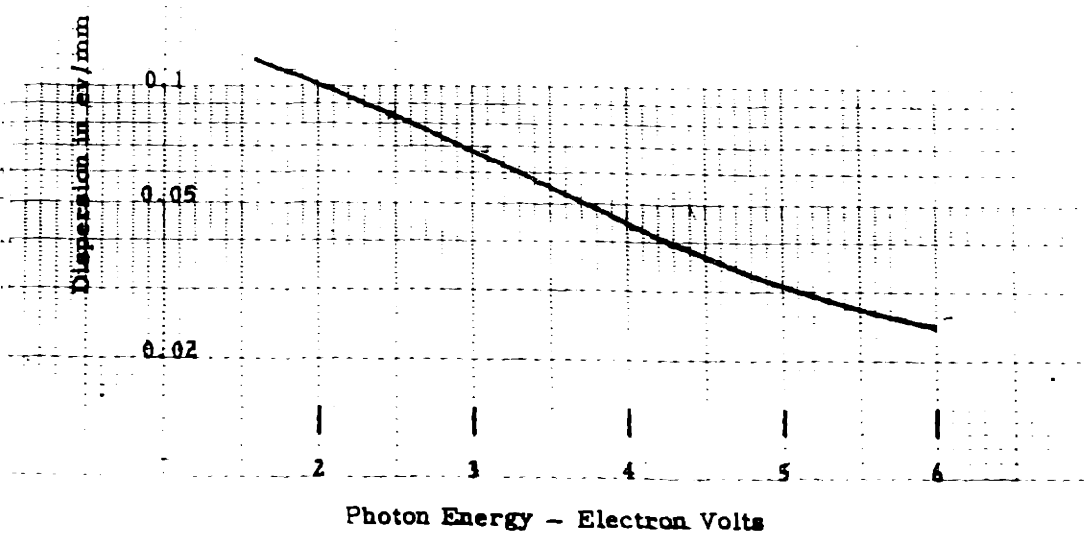
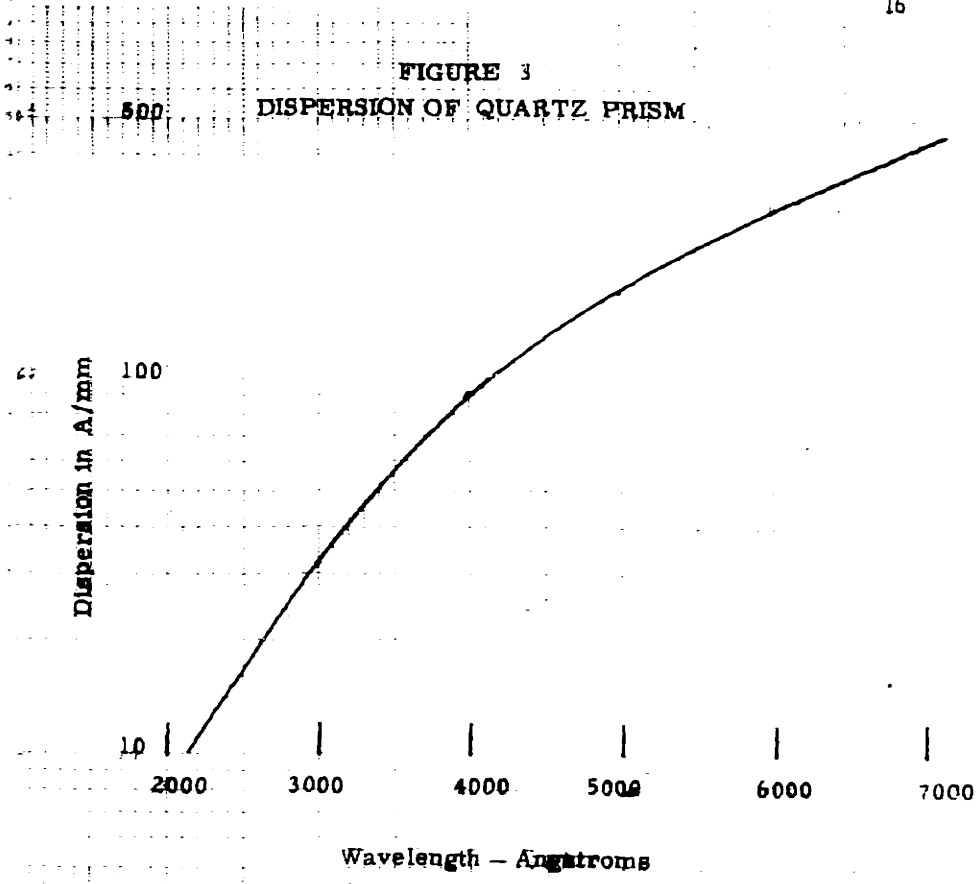


FIGURE 3
DISPERSION OF QUARTZ PRISM

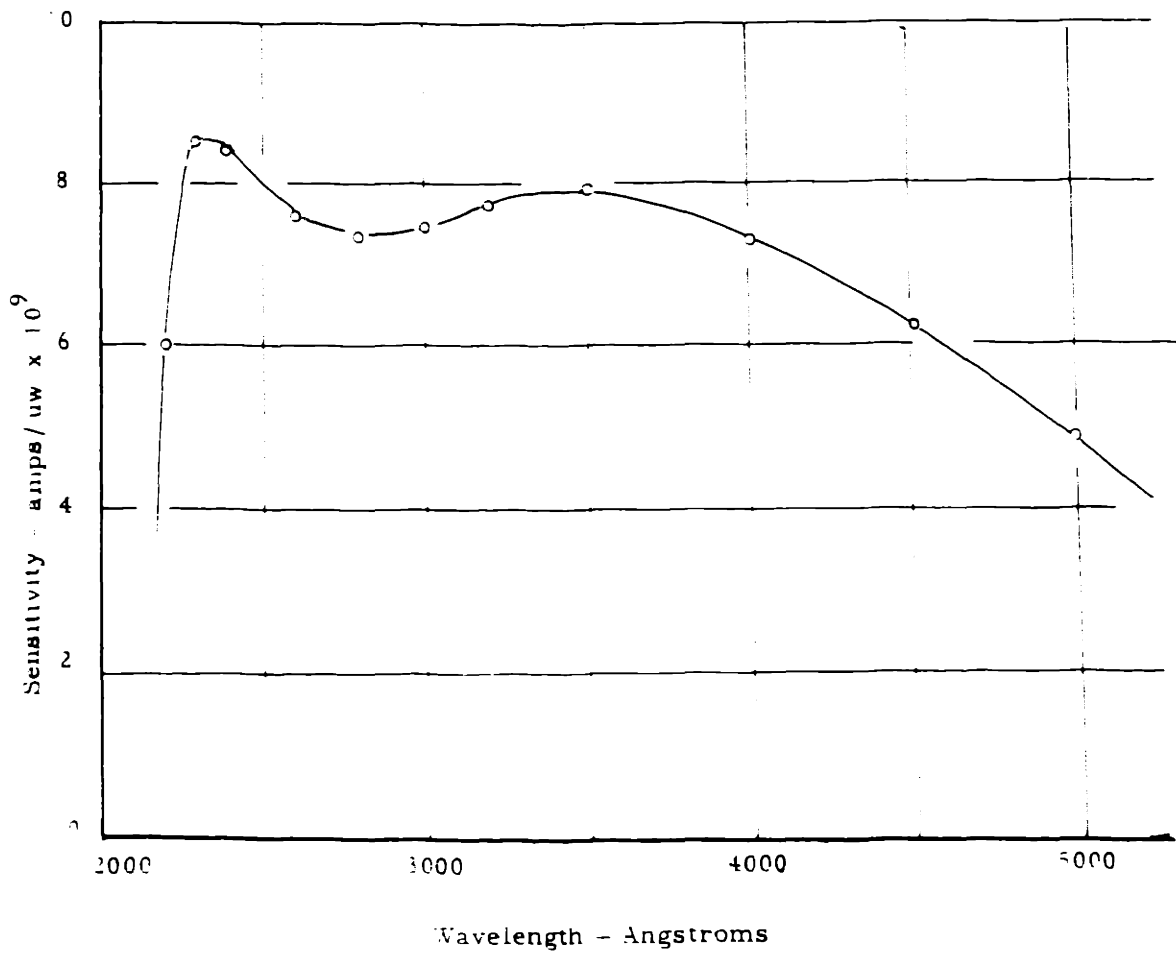


calibrated against a special compensated radiation thermocouple.[†] The calibration of this phototube is given in Fig. 4. The absolute sensitivity of the thermocouple was not known accurately, but the readings are estimated to be correct to 50 per cent. This is about the estimated error in the intensity measurements of the light falling on the sample due both to the reflectivity of the tube window and to the fact that the sample may not intercept all of the light from the monochromator. For these reasons, absolute values of the quantum yield quoted later may be in error by a factor or two, although relative values are accurate to ten per cent.

E. Vacuum Techniques

All the experimental tubes used in this research were pumped on a two-stage mercury diffusion pump system. This consisted of a taper pump, a jet pump with a Welsh Duo-seal fore pump. Pressures were measured with the Bayard-Alpert type of ion gauge⁽²⁸⁾. During some of the work, gauges of the original Bayard-Alpert design were used, but later they were replaced by the modified Bayard-Alpert gauge with an added outside shielding grid. Another modified design, which permitted the gauge to be outgassed by conduction heating rather than by R-F bombardment, was used in some of the tubes. In

[†] I am indebted to Dr. M. A. Gileo for making this calibration.



CALIBRATION OF 935 PHOTOTUBE
FIGURE 4

all cases the gauges were calibrated against a McLeod gauge using dry nitrogen, and the pressures quoted are equivalent to pressures of nitrogen.

Vacuum processing of a tube consisted of two or three overnight bakeouts of the tube at 450° C, with outgassing of the accessible metal parts of the tube and the ion gauge between the bakeouts. Before sealing off the tubes the constrictions in the pumping leads were heated to the softening point and the gas evolved allowed to be pumped out. After sealoff, the ion gauges were run continuously at an electron current of 2 ma to clean up the residual gases left in the tube.

III EXPERIMENTS ON QUARTZ

Quartz was the first material to be studied since the previous work by Jeffries ⁽²⁹⁾ had indicated that its photoelectric threshold was about 4.5 ev. Consequently it was considered that with a refinement of his techniques the spectral distribution of the photoemission could be studied.

A. Samples

Crystalline quartz of optical quality was obtained from the Valpey Crystal Company⁺. Crystals of three orientations were used, X-, Y- and Z-cut, i.e. with the optic axis perpendicular to the plane of the crystal, and two orientations with the optic axis in the plane of the crystal. The fused quartz used⁺⁺ was of clear optical quality, with no faults. All samples were ground to the form of thin discs, .15 to .2 mm thick, and 2 to 2.5 cm in diameter. The surface to be studied was given an optical polish, the other surface being left fine ground.

+ Holliston, Mass.

++ I am indebted to Mr. A.G. Hall for furnishing and preparing these samples.

Quartz is an excellent insulator, with a conductivity at room temperature of 10^{-16} to $10^{-19} \Omega^{-1} \text{cm}^{-1}$. (30) Consequently, photoemission cannot be measured continuously since the surface charges positively to the potential of the surrounding electrodes as electrons are removed by illumination of the surface. For this reason, an electrode was evaporated onto the ground surface of the quartz, and the current to the front surface measured by the amount of charge induced on this back electrode. Measurements were made keeping the back electrode at ground potential and the potentials of all other electrodes fixed. Thus, if C_1 is the capacitance from front to back surface of the crystal, C_2 the stray capacitance of the front surface to other elements in the tube and I_0 the current to the front surface, the measured current I_1 to the back electrode will be

$$I_1 = I_0 C_1 / (C_1 + C_2)$$

The estimated magnitudes of C_1 and C_2 are 50 and $< 10 \mu\text{f}$ respectively, so at least 80 per cent of the current to the front surface will be measured by the electrometer circuit. The resistance from front to back surface is calculated from the conductivity to be 10^{14} to 10^{17} ohms. Thus the time constant for decay of the charge deposited on the front surface is from one hour to 50 days. Thus, except for the lowest resistivity crystals, conductivity through the crystal will not interfere with the measurement at all.

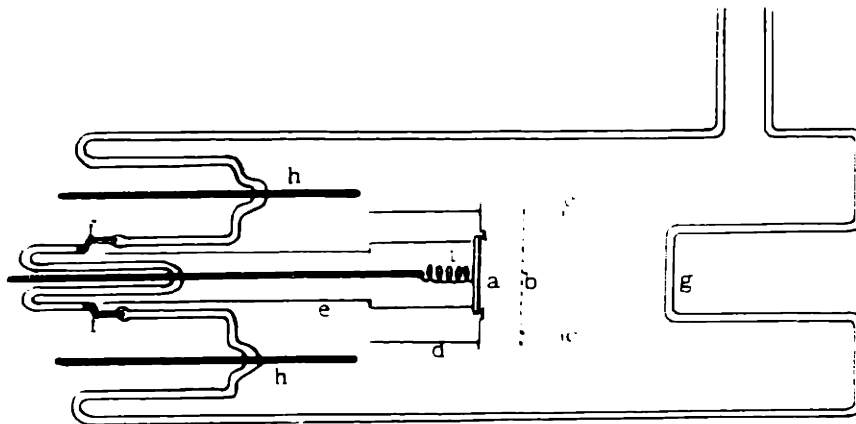
B. Tube Construction

Several designs for tubes were used in this work, new features being added as new shortcomings became apparent. The basic tube design finally used for this work is shown in Fig. 5. After initial difficulties with leakage and polarization currents to the measurement electrode (much of this work was done in the summer under high humidity conditions when the surface conductivity of the glass becomes appreciable), the kovar ring seal (f) was included in the current measuring electrode press. Maintaining this guard ring at ground potential and shielding the glass of this press from high voltages completely eliminated this trouble. The double shield can structure was included in the tube design so that the front retainer shield (d) could be maintained at a potential nearly equal to that of the front surface of the sample while at the same time the back shield can was maintained at such a potential that photoemission from the back electrode was eliminated. This assembly made possible the identification of stray currents, and their reduction to a minimum.

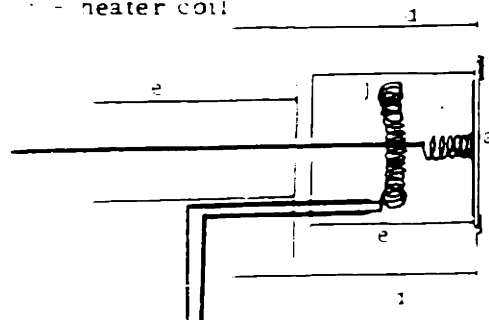
To eliminate photoemission from surface impurities, two methods of cleaning the sample were employed: heating to a high temperature, and bombarding the surface with electrons or ions. At first it was assumed that all samples could be cleaned by heating and some time was spent in finding a suitable design for a radiation oven to do this. In the design of the radiation oven, it was desired to use no insulators to support the heater element

FIGURE 5

EXPERIMENTAL TUBE FOR MEASUREMENT OF PHOTOEMISSION
FROM QUARTZ



- a - sample
- b - collector grid
- c - tungsten filament
- d - retainer shield
- e - back shield
- f - kovar guard ring
- g - quartz window
- h - press leads
- i - spring contact
- j - heater coil



Detail of Radiation Oven for Fused Quartz

since the usual compounds used for this purpose continue to outgas each time they are heated, and thus would contaminate the surface under study. From initial experiments, it was found that an input power of 200 watts was necessary to bring the sample up to a reasonably high temperature ($\approx 1000^{\circ}\text{C}$). This power had to be supplied through press leads of convenient size, limiting the current to not more than ten amperes. In order to have the heater self supporting, use currents of this size, keep the heater cool enough that it would not sag or evaporate, and have a resistance high enough to dissipate the necessary amount of power, a coil of coiled tungsten wire wound on a .100" mandrel was used as the heater. This heater element was flashed to a high temperature after fabrication to recrystallize it and prevent sag after assembly in the final tube. The double shield cans in the tube as described above served also as radiation shields for this oven.

It soon became evident that the crystal quartz samples could not be subjected to cleaning by heating treatment, for they shattered when going through the alpha to beta quartz transition at 575°C . Consequently, they were cleaned by electron bombardment or ion bombardment. Electron bombardment was accomplished by drawing current to the surface from the filament in the tube, depending on a secondary emission ratio of greater than one to keep the surface from charging negatively. In order to bombard the surface with ions, a discharge was maintained in the tube after filling with a few millimeters of argon or helium. The discharge

was maintained for times up to an hour and the gas was then allowed to pump out. This process was repeated several times.

C. Tube Assembly and Processing

Since the metal parts supporting the crystallizing quartz samples could not be outgassed at a high temperature after final assembly without shattering the sample, these parts were given a thorough outgassing before assembly. This consisted of a vacuum firing at 2000°C by induction heating for an hour. Back electrodes of aluminum were used for the crystal quartz, but since the fused quartz was to be heated by a temperature such that aluminum would evaporate at an appreciable rate, tantalum was employed for the back electrode with these samples. Back electrodes were evaporated on in vacuum after etching the sample in hydrofluoric acid for 15 minutes and rinsing in distilled water. Before assembly the front surface was again etched in hydrofluoric acid to remove any contaminants introduced at this stage. To prevent oxidation the tubes were filled with argon while they were sealed together. In some cases it was impossible to outgas the metal parts of the fused quartz tubes after final assembly because the shield cans extended too close to the presses. Then the same procedure that was used for the crystalline quartz tubes was employed. In the other tubes, where the structure allowed, outgassing was done after final assembly.

After assembly and vacuum processing of the tubes, they were sealed off at pressures of about 10^{-9} mm of mercury as measured by the Bayard-Alpert ionization gauge, with the exception of Tube No. 6, on which measurements were made with the tube still on the pumps. The ionization gauges attached to the tubes were run continuously to serve as getters during measurements.

D. Experimental Procedure

The first three attempts to produce tubes were unsuccessful for the following reasons: Tube No. 1 did not have the kovar guard ring included in the current measurement press, and the minimum detectable current was limited to about 10^{-15} amperes. The crystal in this tube was broken in an attempt to clean the surface by heating. Tube No. 2 also employed a crystalline quartz sample. Photoemission was undetectable using the light output of the monochromator, so another attempt was made to clean the surface of this sample by electron bombardment and during the course of the attempt this sample was shattered. Tube No. 3 employed a fused quartz sample, but this tube was made inoperative when a short developed between the heater and the back electrode.

Tube No. 4 again employed a fused quartz sample, and was of the design described in Section B., with a radiation oven for heating the sample and kovar guard ring to reduce leakage

currents. This tube was sealed off the pumps at a pressure of 5×10^{-9} mm Hg, and on standing with the ion gauge running, the pressure came to an equilibrium value of 3×10^{-9} mm Hg. During heating of the radiation oven the pressure rose to 7×10^{-8} mm Hg but upon cooling returned to its equilibrium value of 3×10^{-9} mm Hg. Under direct illumination from the CH-3 source the photoemission measured was 1.12×10^{-13} amperes. With light from the monochromator, no photoemission could be detected, although the current sensitivity was increased to 5×10^{-17} amperes by shielding and by using the capture-of-charge method of current measurement. Such a current is equivalent to a quantum yield of sensitivity of 1×10^{-9} electrons per quantum at 4.65 eV and one of 10^{-7} electrons per quantum at 5.26 eV with the available light intensity. From later work it can be inferred that with the intensities obtainable from the monochromator the photoemission would have been well below this detection limit of 10^{-17} amperes.

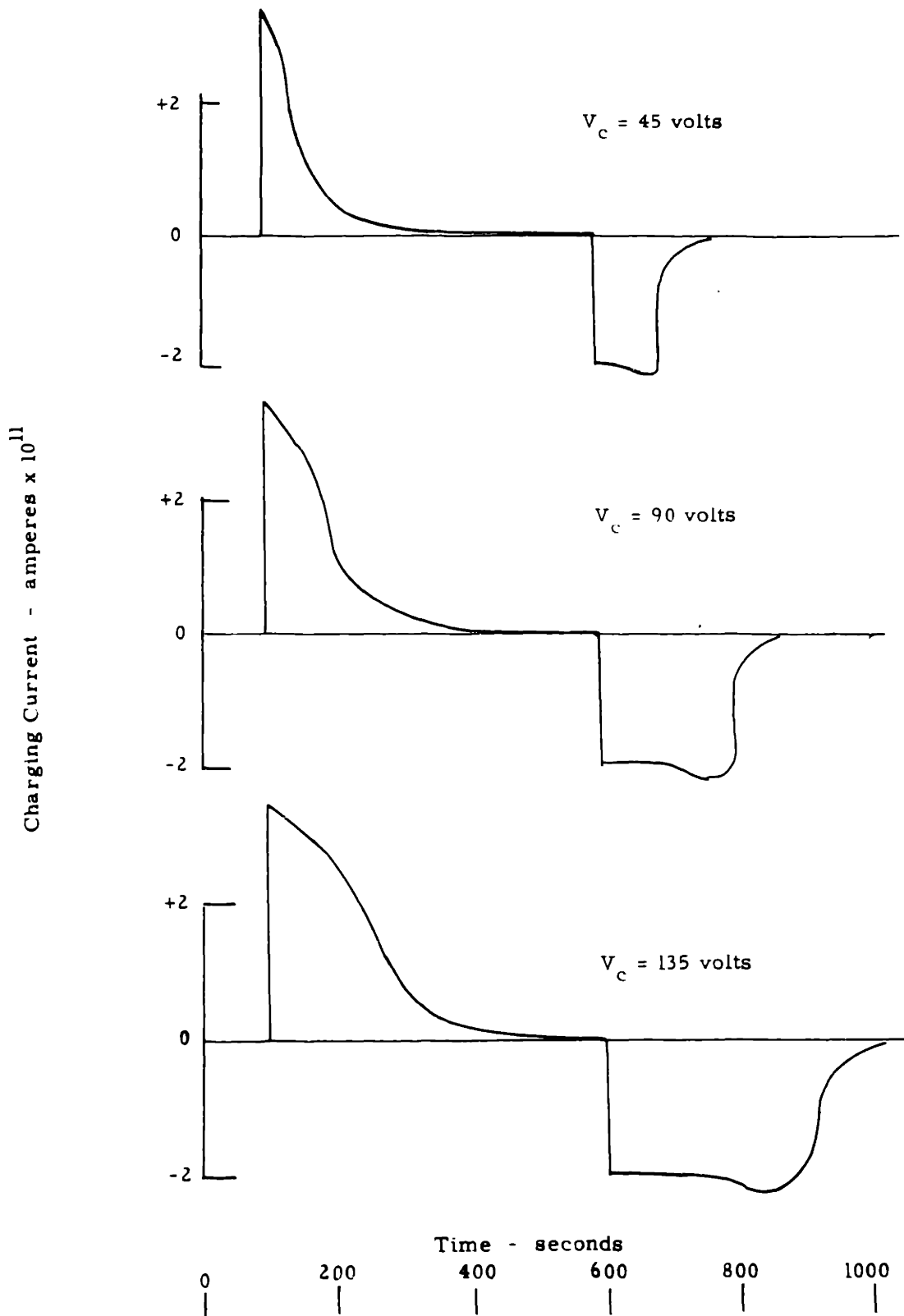
The photocurrent from this sample was studied as a function of the charge on the surface. The surface was charged to the potential of the tungsten filament in the tube by heating this filament until the total emission from it was of the order of 10^{-6} amperes. The charging of the surface introduced no significant change in the photoemission from the surface, as long as the collector potential was maintained at a constant voltage with respect to the surface. At low collecting voltages, the emission current dropped off, indicating that the collection efficiency was falling, i. e. that some of the electrons emitted from the sample were

returned to the sample due to the field configuration. The collection efficiency did not saturate until the collector voltage was of the order of 30 volts.

Since the results of Jeffries indicated that the photoemission from crystalline quartz should be of the order of 10^{-13} amperes at 4.6 to 5.0 eV with the intensities available from the monochromator, it was thought that there might be an essential difference in the character of the photoemission from these two modifications. For this reason, the next tube constructed (No. 5) employed a crystal (X-cut) sample. Construction of this tube was similar to Tube No. 4, except that the heater for the radiation oven was omitted. After vacuum processing, an attempt was made to outgas the surface by drawing electron current to it from the filament in the tube. This tube was sealed off at 8×10^{-9} mm Hg, and with the ion gauge running reached an equilibrium pressure of 4×10^{-9} mm Hg.

Under full illumination by the CH-3 lamp, the emission from this sample was 2×10^{-10} amperes. This emission was high enough that the time-current curves for charging and discharging the surface of the quartz were easily observed. These are shown in Fig. 6. After the tube had been illuminated with all elements grounded for a long time, so that the surface had come to ground potential, the light was turned off, and the collector voltage switched positive. When the light was turned on, a current pulse was measured which dropped to zero after the surface had been charged to the collector potential. When the collector voltage was returned to ground, a

FIGURE 6
CHARGING AND DISCHARGING CURVES
Tube No. 5



current pulse in the opposite direction was observed, starting with an initial value different from that of the changing pulse but persisting until the total charge transferred the same, indicating that the front surface had returned to ground potential. The charge transferred was determined by measuring the areas under the current-time curves, and is shown in Table I.

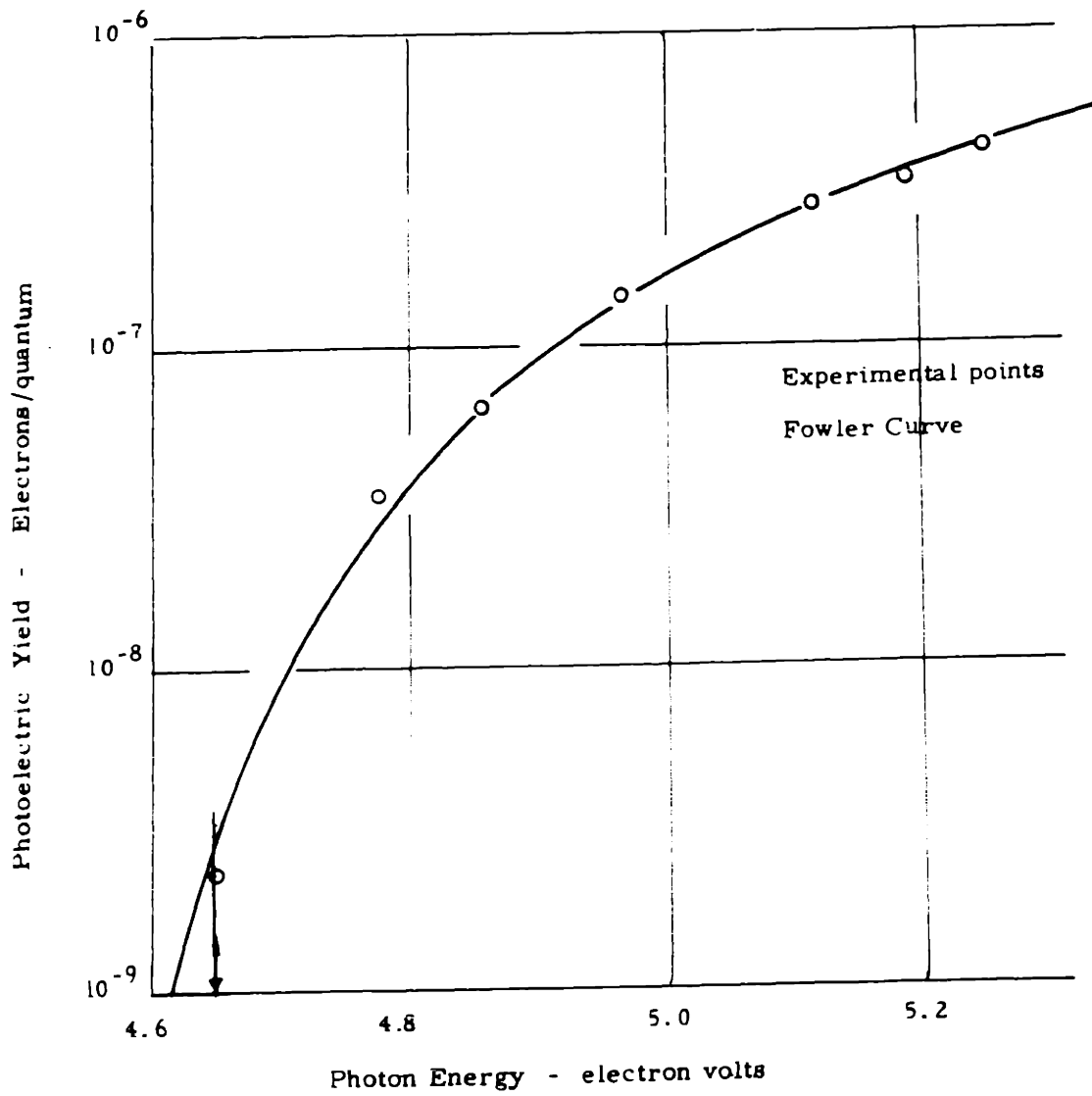
TABLE I

Collector voltage	Charge transferred on	Charge transferred off
45 volts	2.45×10^{-9}	2.5×10^{-9} coulombs
90	4.95	4.90
135	7.50	7.40

From these numbers, the capacitance which was being charged may be calculated to be 53.2 μf . From the dimensions of the sample, assuming the active area to be 1.8 cm diameter, thickness .2 mm, the capacitance is calculated to be 57 μf . The difference of these two numbers leads to a calculated stray capacitance of the front surface to ground of the right order of magnitude.

Because of these changing and saturation effects, it is clear that the photoemission measured came from the quartz sample and not from other parts of the tube. The spectral distribution of the photoemission from this sample is shown in Fig. 7. The data fits a Fowler plot well over the range for which data were taken, with a work function of 4.65 volts.

FIGURE 7
SPECTRAL DISTRIBUTION OF PHOTOEMISSION Tube No. 5



An attempt was made to observe a shift of the photoelectric threshold with the amount of surface charge in order to determine the density of surface states . (See Appendix I) The surface was charged to 500 volts and the spectral distribution again determined. No significant shift was noted, indicating that the surface state density was greater than $10^{13} / \text{ev-cm}^2$.

In the light of this result, the processing of the tube was reexamined with the suspicion that the surface might have been contaminated. From the vapor pressure of tungsten ⁽³¹⁾ it was calculated that an appreciable fraction of a monolayer of tungsten was deposited on the surface of the quartz during the electron bombardment for outgassing. For this reason, it was decided to reclean this sample of quartz and repeat the experiment.

The tube was cracked open and the surface etched again for 15 minutes in hydrofluoric acid. After this treatment the tube was reassembled and pumped. After sealoff, the equilibrium pressure with the ion gauge running reached 5×10^{-9} mm Hg. After this treatment, the emission from the surface of the sample was 3×10^{-13} amperes under full illumination by the CH-3 mercury arc. This is lower than the previous emission by a factor of 600, and was so low that the spectral distribution of the photoemission sample could not be determined. It was concluded that the photoemission from this sample observed previously was due to contamination of the surface with tungsten. A further check was made on this hypothesis by evaporating an estimated 1/10 monolayer of

tungsten on the surface and again measuring the photoemission from the surface. This treatment increased the yield under full illumination by the CH-3 factor of 100, and made it possible to measure the spectral distribution of the photoemission. The charging and discharging curves for the sample were similar to those observed previously, but since the maximum current was smaller by a factor of 10, they persisted ten times as long, transferring the same amount of charge to the surface as before. The currents measured to determine the spectral distribution of the photoemission were of the order of 5×10^{-16} amperes. These data are plotted in Fig. 8. A Fowler curve fitted to these data indicates a work function of 4.55 volts. Attempts to measure the density of these extrinsic surface states by the method described above were unsuccessful, because the necessary high potentials introduced noise in the measurement circuit of the same order of magnitude as the current to be measured.

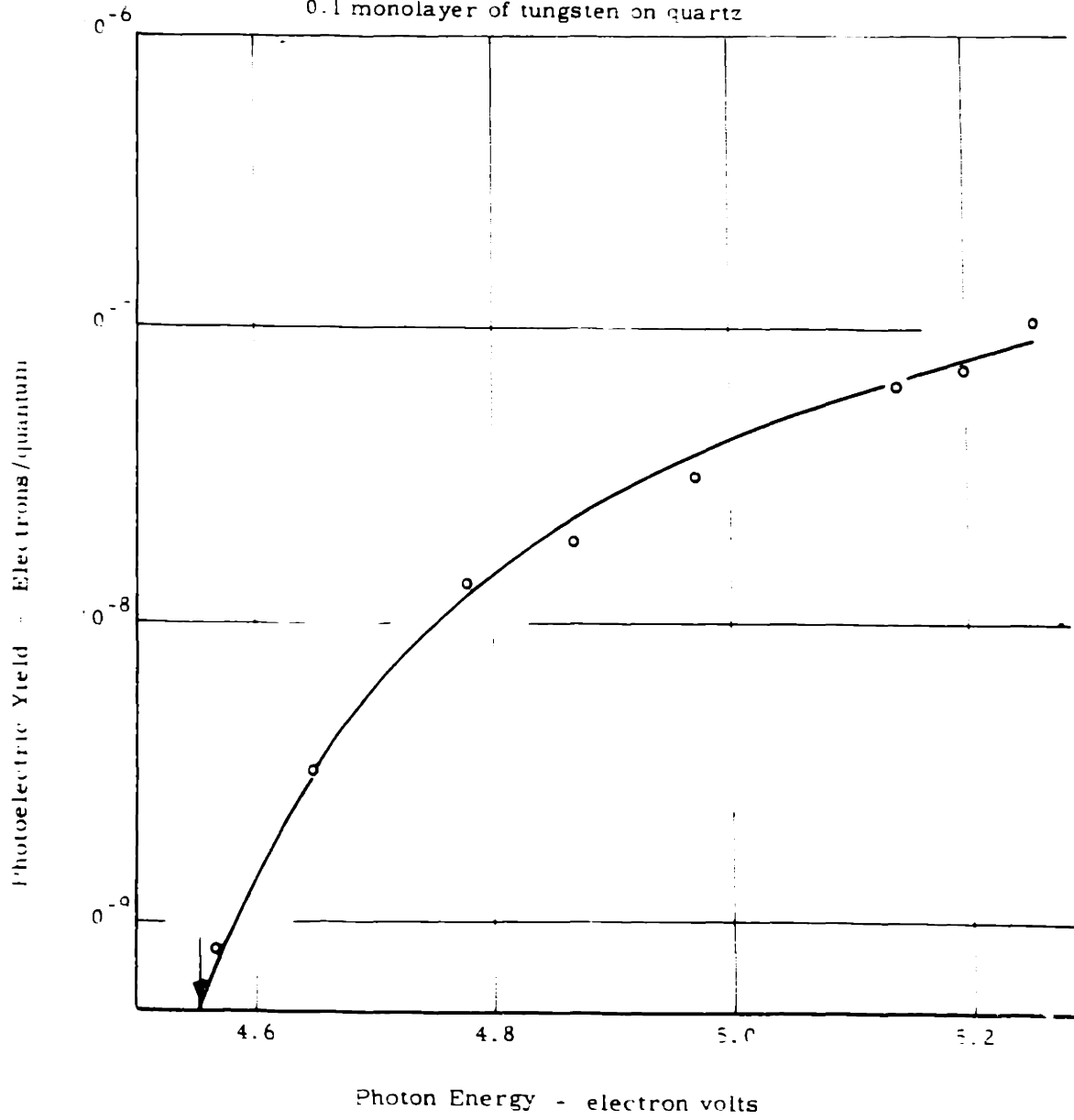
The surface and volume conductivity of this sample, even in its original contaminated state, was such that if the surface were charged, 80 per cent of the charge deposited remained after waiting a period of 60 hours. This was determined by measuring the charge transferred upon discharging the surface.

Tube No. 6 was the same in construction as Tube No. 5. The sample in this tube was a Z-cut crystal, and measurements were made with the tube on the vacuum system so that the variation of the photoelectric yield could be studied as a function of the gas contaminants on the surface.

FIGURE 8

SPECTRAL DISTRIBUTION OF PHOTOEMISSION Tube no. 5

0.1 monolayer of tungsten on quartz



After the tube had been pumped to a good vacuum, the photoemission was measured under full illumination to be 1×10^{-13} amperes. This was increased to 3×10^{-13} amperes by exposing the surface to a discharge in argon for five minutes, and pumping out. Exposing the surface to a discharge in oxygen reduced the emission to 9×10^{-14} amperes. A hydrogen discharge brought the emission level back to 1.5×10^{-13} amperes. This cycle was reproducible to within 50 percent.

The tungsten filament in the tube was then flashed in order to deposit 1/10 monolayer of tungsten on the surface as in the previous tube, and the experiments on the effect of exposing the surface to discharges in various gases were repeated. The results are shown in the following table.

Surface treatment	(Quartz with .1 monolayer of tungsten)	(Clean quartz)
Initial emission	3×10^{-11} amps	1×10^{-13}
Discharge in argon for 5 mins.	2.5×10^{-11}	3×10^{-13}
Discharge in oxygen for 15 secs.	8.0×10^{-14}	9×10^{-14}
Discharge in hydrogen 15 secs.	2.0×10^{-11}	1.5×10^{-13}

These results indicate that it is possible to affect the photoemission to a great extent by the surface contaminants, and thus emphasizes that great care must be taken if a surface characteristic of the pure substance is to be studied. For this reason, and since the photoemission from clean quartz was well below the limit

of detection for spectral distribution measurements, it was decided that another material should be studied with the hope of finding a material which had a lower photoelectric threshold and/or higher quantum yield.

In this study of the photoemission from quartz, it was noted that on turning on the light, a short pulse of current flowed in the positive direction (corresponding to electrons leaving the surface) and a short pulse of current flowed in the negative direction upon turning off the light. Under full illumination by the CH-3, the peak current for this effect was of the order of 10^{-13} amperes, and the total charge transferred was about 10^{-12} coulombs. This effect persisted and was independent of potentials in the tube. It was thought possibly due to photoemission into the quartz from the aluminum back electrode, and was studied quite carefully for it might furnish a determination of the electron affinity of quartz. The study of this effect showed that it was proportional to the light intensity, and extended to at least .5 ev (24000 A). When it was noted that the magnitude of the effect was approximately proportional to the photon energy, heating of the sample was thought to cause the effect. This hypothesis was proved by "illuminating" the surface with a container of liquid air, and finding that the effect is reversed.

It is estimated that under full illumination radiant energy of 0.1 watts is incident upon the crystal, giving an induced charge of about 10^{-12} coulombs or giving an induced voltage of .02 volts across the crystal. The temperature rise calculated for this

amount of radiant energy is of the order of 30° C. If the effect noted is to be explained by the absorption of the radiation by the back plate and consequent heating of the quartz near the back plate, a negative thermoelectric power of 1 millivolt/degree can easily account for the effect.

E. Summary of Results

An upper limit on the photoelectric yield from clean quartz of 10^{-9} electrons per quantum at 4.65 ev, and of 10^{-7} at 5.26 ev was established. Gas contaminants on the surface could vary the total emission under illumination by a CH-3 mercury arc by 50 percent.

It was shown that a fraction of a monolayer of tungsten on the surface would increase the yield by a factor of 1000, and that the spectral distribution of photoemission from the surface then closely follows the Fowler theory, with a work function of 4.55 to 4.65 ev. An attempt to measure the density of states thus introduced was unsuccessful, indicating a surface state density of greater than 10^{13} / ev-cm². After depositing a fraction of a monolayer of tungsten surface the yield could be decreased by a factor of 300 by exposing the surface to oxygen, and nearly restored to its original value by exposing the surface to hydrogen, thus exhibiting the behavior of metallic tungsten. The surface conductivity remained low, however, as indicated by the fact that a charge deposited on the surface would remain for several days.

IV EXPERIMENT ON MAGNESIUM OXIDE

A. Samples

Single crystals of magnesium oxide were obtained from the Norton Company[†]. From the large crystals supplied, samples were cleaved to approximately .05 x .5 x 1.5 cm. As in the case of quartz, a tantalum electrode was plated on one side of the crystal, for the measurement of the photoemission by the induced charge method. The samples were cleaned by rinsing in alcohol and distilled water before assembly into the experimental tube.

For the work on powdered magnesium oxide, the samples were prepared by pyrolysis of magnesium carbonate. The magnesium carbonate was deposited on a platinum ribbon from a suspension in distilled water. The platinum ribbon served as a heater for the pyrolysis of the magnesium carbonate, and during the photoemission studies as the current measurement electrode.

B. Photoemission from Single Crystal Magnesium Oxide

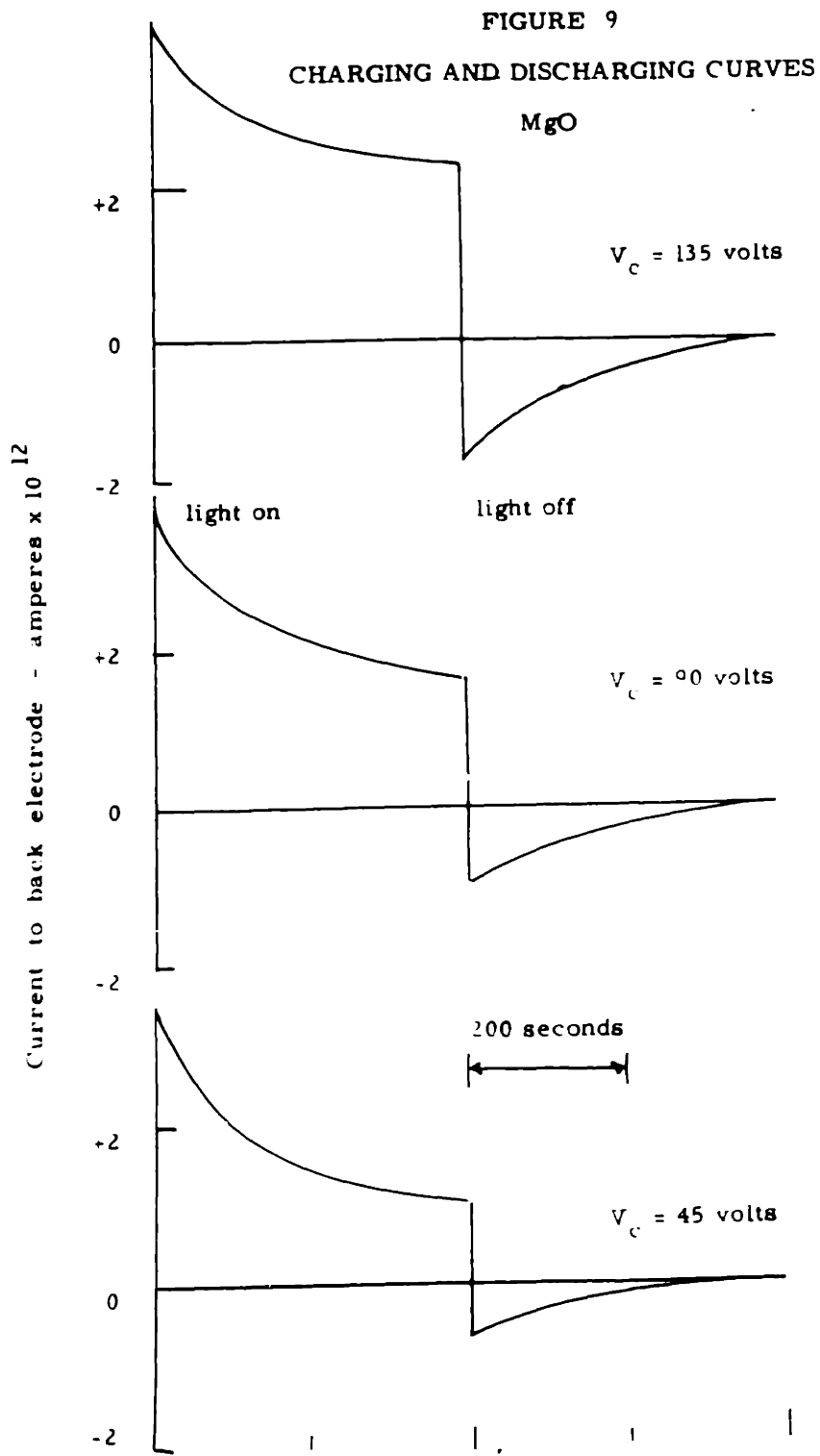
The tubes used for the study of the photoemission from

[†] The Norton Company, Niagara Falls, N. Y.

magnesium oxide were similar to those used for quartz, with the exception that the sample holder was rectangular, not round. A radiation oven was included in the tube. The first tube assembled developed a short circuit between the heater and the measurement electrode, and consequently had to be cracked open and reassembled. After vacuum processing, the tube was sealed off at a pressure of 10^{-8} mm Hg, and came to an equilibrium pressure of 7×10^{-9} mm Hg.

The resistivity of the crystal was much lower than that for the quartz, the resistance from the back electrode to the front retainer shield being about 5×10^{11} ohms. As a result of such high conductivity, the sample could not be charged in the manner used with the quartz, and measurements had to be made with the front electrode maintained at ground potential to eliminate spurious conduction currents.

On illuminating the crystal with the CH-3 mercury arc, the photocurrent had an initial maximum value of about 4×10^{-12} amperes, decaying in 200 seconds to a value dependent on the collector voltage. When the light was turned off, the current being measured reversed direction, and again after about 200 seconds decayed to zero. These charging and discharging curves are shown in Fig. 9. These curves are explained in the following way. If C_1 is the capacitance across the crystal and C_2 the stray capacitance from the front surface to other electrodes in the tube, the current registered by the back electrode, for no conduction through the crystal, will be $I_0 C_1 / (C_1 + C_2)$ where I_0 is the current to the front



surface. If there is nonconduction current present, the fraction $C_2/(C_1 + C_2)$ of it will be registered in addition to the other current. When the sample is illuminated, with the front surface at ground potential and there will be no conduction current initially. After some charge has been removed from the surface, a potential will be developed across the crystal, and conduction current will start to flow. Also, as the surface charges positively, the collection efficiency for emitted electrons will decrease since the front retainer shield, which is maintained at ground potential, will present a retarding field through which the electrons must go before reaching the anode. The final steady state will be determined by the relative magnitudes of these effects. Estimating a rising fraction of the current registered to be due to conduction, we may calculate the amount of charge under the peak of the emission current vs. time curve to be about 2×10^{-10} coulombs for a collector voltage of 45 volts. If it is assumed that the front surface has charged almost to the collector potential, the capacitance across the crystal is calculated to be 4.5 μpf , which is approximately equal to that calculated from the dimensions of the sample.

When the light is turned off, the current registered on the back electrode reverses sign. This indicates that the potential of the front surface is not returning to zero by means of conduction current from the back electrode, for such a current would flow in the same direction as the current under illumination. We must conclude that this charge is leaking onto the surface from the front

retainer shield by surface conductivity, or at least that such an effect is larger than that due to conductivity through the sample. This surface conductivity would also decrease the current measured to the back electrode during illumination and photoemission, but to a limited extent since in this case the conductivity of the crystal is much higher due to photoconductivity in the bulk.

Day ⁽³²⁾ quotes values of induced photoconductivity of $10^{-11} \Omega^{-1} \text{cm}^{-1} \text{watt}^{-1}$ in the visible and near ultraviolet, which is sufficient to be consistent with this explanation. He also states that the conductivity of compressed pills of powdered magnesium oxide have dark conductivities a million times greater than for single crystals of the same dimensions, indicating high surface conductivities of magnesium oxide.

The photoelectric yield from the single crystal of magnesium oxide, while ten times larger than that for quartz, was still below the detection limit of the system for the determination of the spectral distribution of the photoemission. Work with filters indicated that the threshold was about 4 eV; a clearer determination of the spectral distribution from this sample was impossible. Although small currents, near the detection limit of the electrometer, could be detected using the light outputs of the monochromator, it was felt that the currents could be arising from spurious effects such as photoconduction, or polarization, so attention was turned to work on powdered samples. A much larger surface area of the material may be illuminated using a powdered sample at

nearly the same intensity as for the single plane surface. This is due to the multiple reflections in the powdered sample combined with the low absorption in the wavelength range of interest in this study. Thus larger quantum yields were obtained since photoemission is a surface effect.

It was evident at this time that a more intense source was necessary for this work, so the AH-6 high pressure mercury arc was employed for the study of powdered magnesium oxide. With this source, the photocurrents were conveniently large for measurement with the vibrating reed electrometer by the constant deflection method.

C. Photoemission from Powdered Magnesium Oxide

Because of the higher conductivity of powdered magnesium oxide, the tube for work on this substance was designed to have conduction through the sample provide the necessary current for photoemission, instead of using the induced charge principle. A thin coating of magnesium carbonate was deposited on a platinum ribbon from suspension in distilled water to serve as the cathode of the tube. Platinum was used because it is a refractory metal and because of its high work function (~ 6 volts) so that results would not be hampered by photoemission from the cathode support. The ribbon was mounted on the two lead center press with a kovar guard ring to eliminate conduction currents. The shield can, used to eliminate electrostatic pickup, had an opening in the front end

3 mm x 18 mm to expose the active surface. The electron collector was made of tantalum sheet with a somewhat larger opening through which the cathode was illuminated. This tube is shown in Fig. 10.

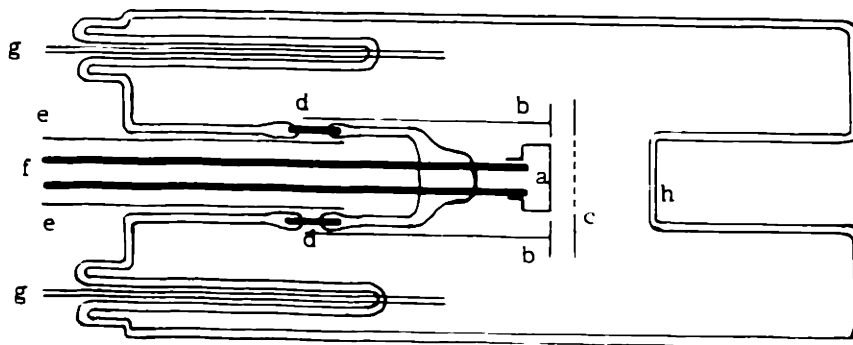
Since the first tube assembled had a pyrex window, studies of photoemission were limited to wavelengths longer than 3100 Å. The H-6 source was not yet available, and work was limited to the study of total emission from the magnesium oxide under direct illumination by the CH-3 mercury arc. No measurements of the spectral response were made. This tube was used to determine the processing which would have to be used to obtain stable emission from magnesium oxide.

It was expected that higher quantum yields could be obtained by using powdered samples with large surface area. It has been shown that the particle size obtained by pyrolysis of magnesium carbonate increases with increasing annealing temperature (33, 34). Thus, ^{higher} quantum yields were expected for samples which had been annealed at low temperatures, but the effect found was the opposite of this, as shown in Table III.

TABLE III

Annealing Temperature	Photoemission current
before breakdown (MgCO_3)	$< 10^{-15}$ amperes
390°C	5×10^{-14}
450°C	5×10^{-13}
750°C	7×10^{-13}
900°C	1.2×10^{-12}

FIGURE 10
 EXPERIMENTAL TUBE FOR MEASUREMENT OF PHOTOEMISSION
 FROM POWDERED MgO



- a - platinum ribbon .002" x 2 mm
- b - tantalum shield can
- c - tantalum anode
- d - kovar guard ring
- e - external shield can
- f - 0.050 " tungsten heater leads
- g - press leads for other elements
- h - fused quartz window

If the effect of higher emission from the cathode for smaller particle size was present, it was masked by another effect which increased the emission after higher annealing temperatures were used. This effect may be the driving out of breakdown products, for it was noted that the pressure in the tube rose significantly each time that the temperature of the cathode was increased, although the conversion to magnesium oxide is supposed to occur at 450° C.

After annealing the sample at the higher temperature, a decay of the photoemission was noted upon illumination, perhaps due to the depletion of the traps from which the emission was arising. This decay took place over about 200 seconds, decaying to ten percent of its value after that time, and remaining steady thereafter. The decay was slower for lower light intensities, and the emission could be restored to its initial value by flashing the cathode to a high temperature.

It was noted that the photoemission varied with the temperature in a way to suggest that the work function was increasing with increasing temperature. The sample was first flashed to 5 amperes for thirty seconds to increase the conductivity and neutralize the sample, then held for thirty seconds at the temperature at which the measurement was to be made, and then illuminated. The results are shown in Table IV.

TABLE IV

Photoemission from MgO as a Function of Temperature

Heater current	Temperature	Emission current
0	20°C	3.2×10^{-13} amperes
1 ampere	80°	2.4
2	175°	1.0
3	340°	1.3
4	555°	4.0
5	730°	17.
6 ⁺	870°	35.

+ At 870°C the cathode emitted thermionic current of 25×10^{-13} amperes

The trend of these values indicates that the photoelectric threshold is increasing with temperature, the rising emission at the higher temperature being due to a rapidly increasing population in the conduction band. The rising threshold indicates that the Fermi level is falling with increasing temperature, which is expected if the Fermi level lies above the middle of the forbidden band as is indicated by later data.

The second tube constructed employed a quartz window, and by using the more intense AH-6 source, a detailed study could be made of the spectral distribution of the photoemission.

During vacuum processing, the carbonate was broken down at a temperature of 900°C for ten hours. The photoemission from

the sample when illuminated directly with the CH-3 mercury arc showed the same decreasing emission as the temperature was increased until the thermionic range is approached as did Tube No. 1, but with a smaller percentage variation, presumably due to the larger range in wavelengths transmitted through the quartz window. These data are shown in Table V.

TABLE V

Photoemission from MgO vs Temperature Tube No. 2

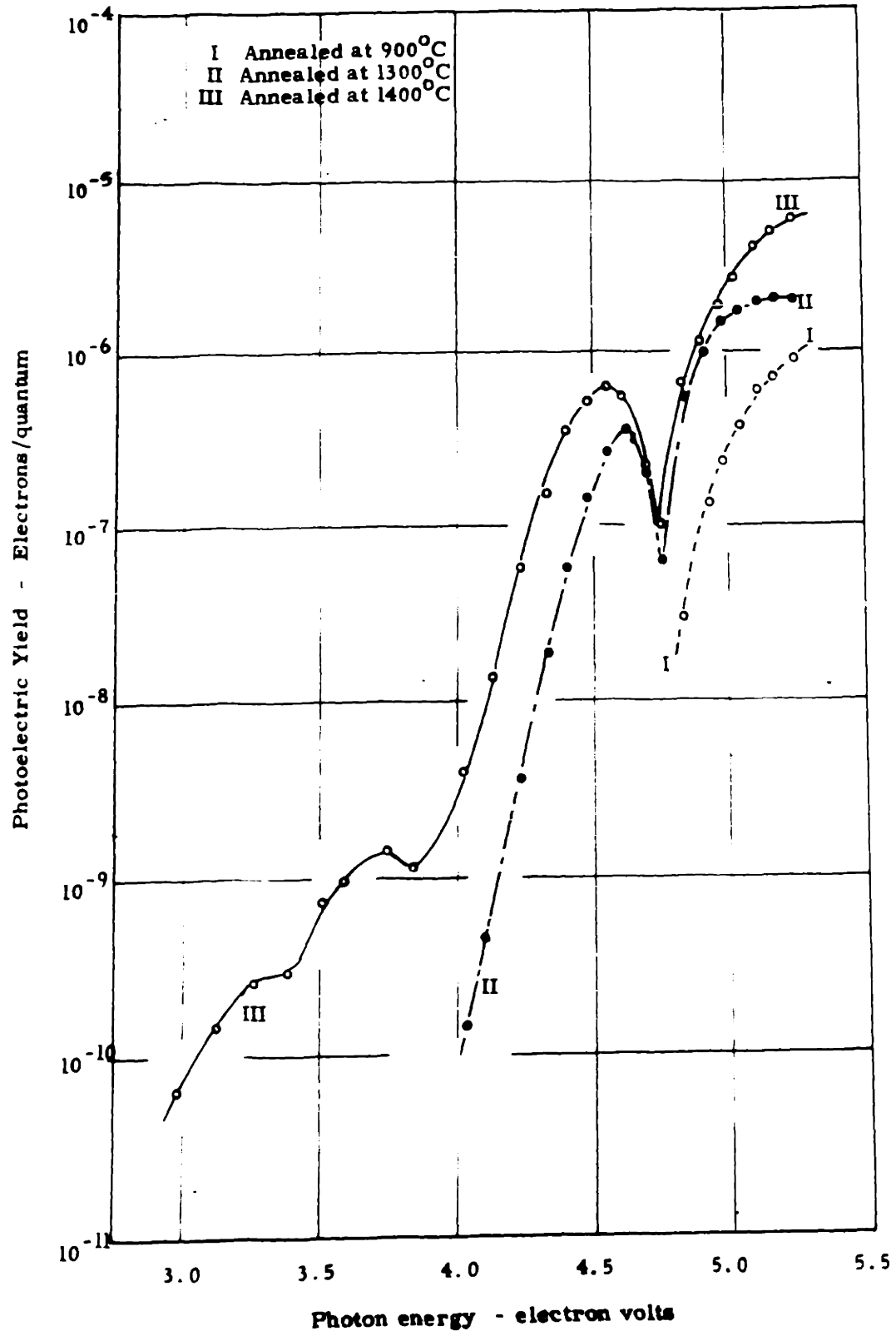
Heater current	Temperature	Emission current
0 amperes	20 ^o C	6.4 x 10 ⁻⁸ amperes
1	100 ^o	5.8
2	350 ^o	5.6
3	650 ^o	5.2
4 ⁺	900 ^o	7.0

⁺ Thermionic emission of 8×10^{-12} amperes

The spectral distribution of the photoemission from this tube was measured after various annealing temperatures were used. These data are shown in Fig. 11. Curve No. I was taken after the sample was annealed at 4 amperes (900^oC), curve II was taken after flashing the cathode to 1300^oC for ten minutes. Curve III was taken after the sample had been annealed at 1400^oC for two hours. These curves show the activation taking place which was noted in the first tube, i. e. the higher yield

FIGURE 11

PHOTOELECTRIC YIELD FROM MgO Tube No. 2

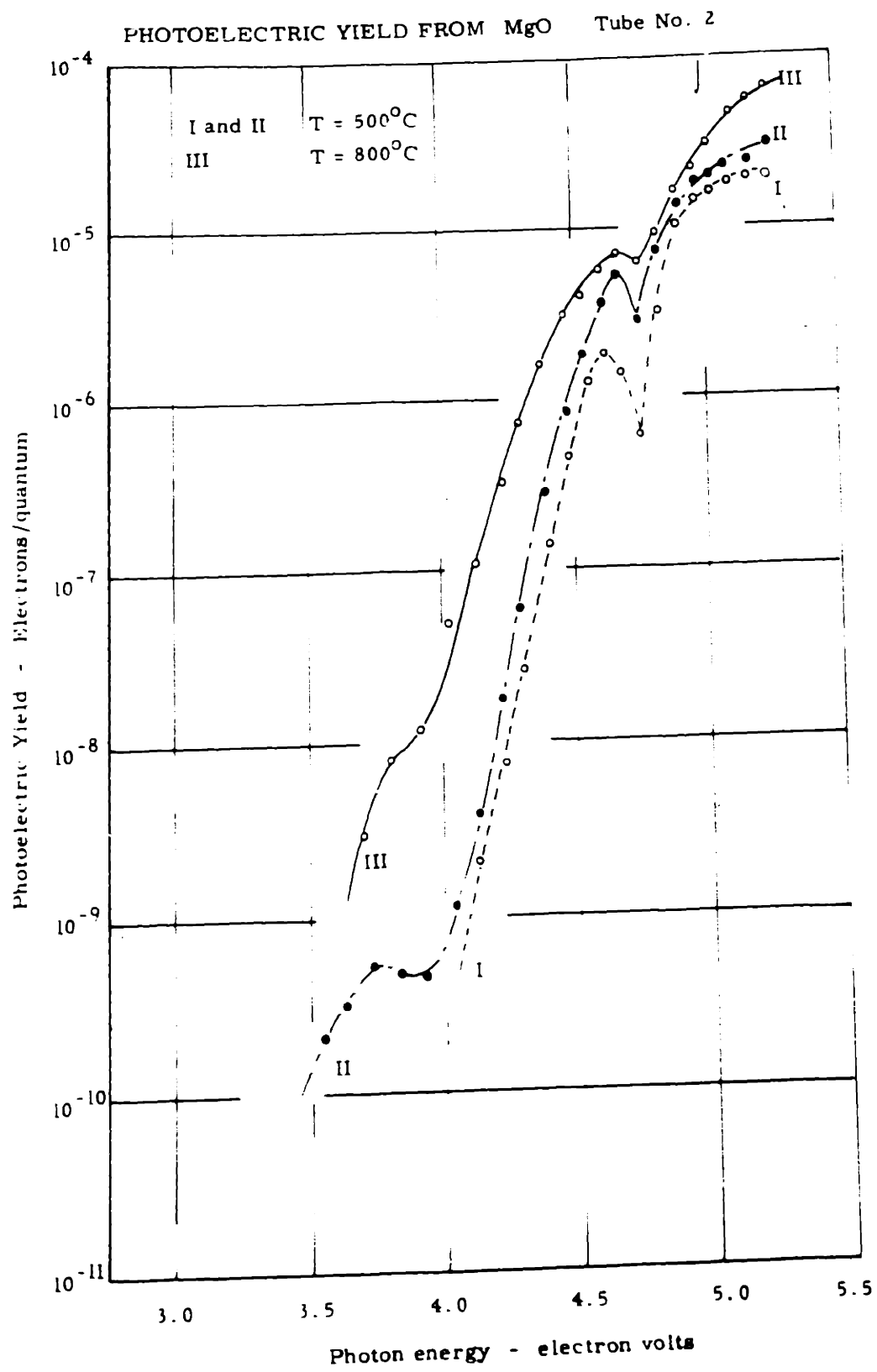


after annealing to the higher temperature. The structure of these curves was quite surprising but was quite reproducible, except for the lowest peak which decayed with time after flashing.

Since it had been noted that the emission varied with the temperature of the cathode, it was desired to measure the spectral distribution of the photoemission at different temperatures. This presented a problem, in that for the measurements of the small currents, the batteries used to heat the filament had to be very well insulated and shielded. It was found, within experimental error, that at room temperature the current to the anode was equal to that measured from the cathode, i. e. that the emission from the tantalum shield can was small compared to that from the magnesium oxide. Since the photoelectric threshold of tantalum is greater than 4 ev, and the scattered light on the tantalum is of low intensity, it was assumed that at the elevated temperatures at which the emission from magnesium oxide decreased, the emission from the tantalum would still be small compared to that from the magnesium oxide. With these considerations, the spectral distribution of the photoemission from magnesium oxide at the higher temperatures was measured at the anode, not at the cathode, of the phototube. The results are shown in Fig. 12.

Curve I shows the photoemission at 2.5 amps heating current (500°C), before the cathode had been annealed at 1400°C . Curve II is the emission at the same temperature after annealing at 1400°C for two hours. Curve III is the photoemission at 4 amps heating current (800°C) in the presence of 5×10^{-13} amperes

FIGURE 12

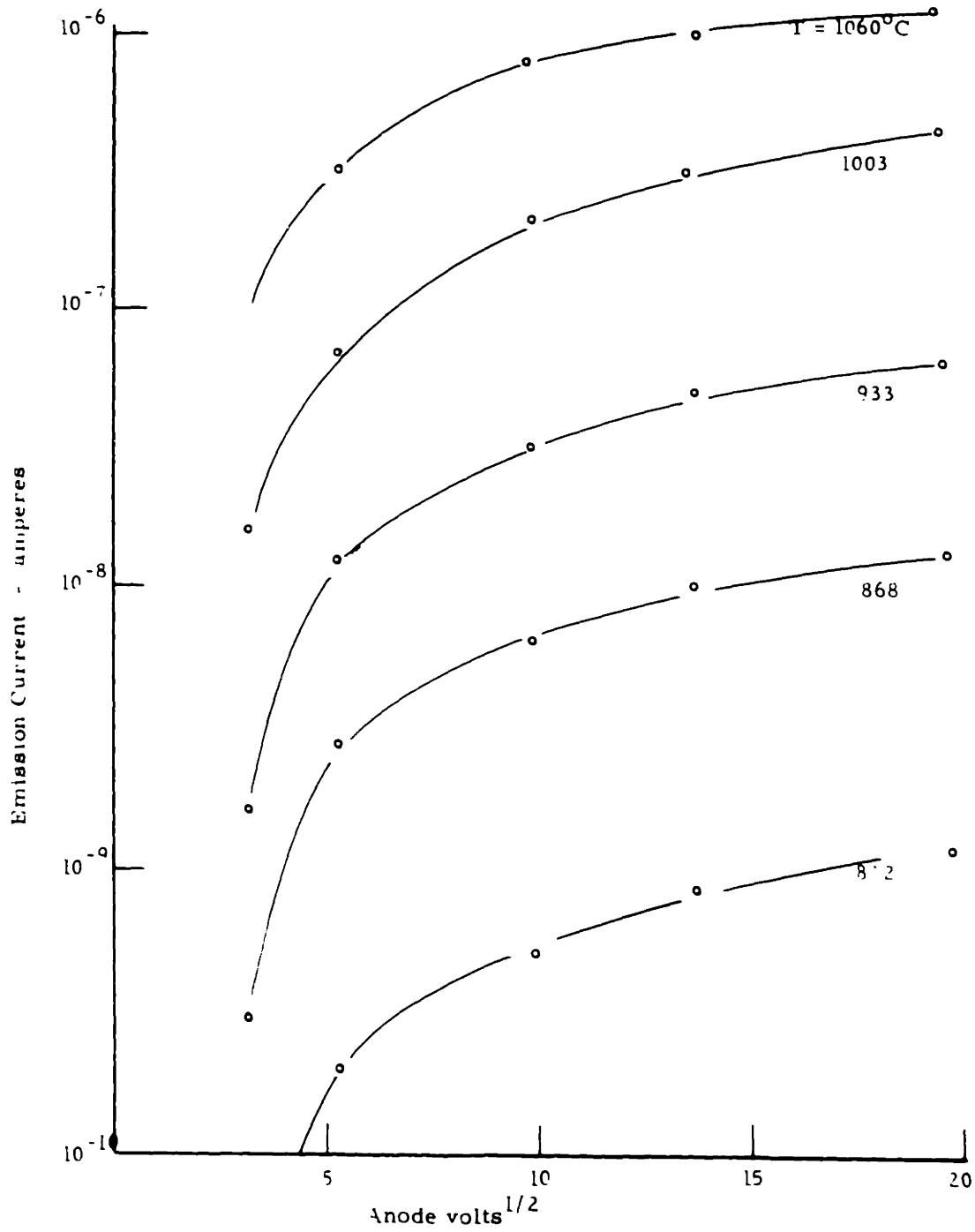


thermionic current. These curves show in more detail that which was inferred from the measurements made without the monochromator. The emission for low photon energies at 500°C is lower than at room temperature, then increases with temperature in the thermionic range. Note too that the structure of the curve smoothes out at the higher temperatures, the decrease in the emission at a photon energy of 4.8 ev nearly disappearing at the higher temperature.

Tube No. 3 was constructed with a Pt - Pt 10 percent Rh thermocouple welded to the platinum ribbon for temperature determinations, so that the thermionic work function of magnesium oxide could be determined. This tube had no quartz window, so the spectral distribution of the photoemission was not determined. The sample was held at 1000°C for 18 hours for initial breakdown of the carbonate before any measurements were made. Initial thermionic data taken on the tube showed activation taking place during the measurements, i. e. the emission was rising with time and was not reproducible. In order to stabilize the emission the cathode was held at 1400°C for one hour, during which large amounts of gas were evolved from the cathode. After this treatment the thermionic emission remained quite stable.

Figure 13 shows the dependence of the thermionic current on the anode voltage. These data show that the emission current begins to saturate at 100 volts if the field dependence of the thermionic emission is neglected. To simplify the data taking procedure, the value of the emission current at an anode potential of 500 volts

FIGURE 13
FIELD DEPENDENCE OF THERMIONIC EMISSION



was used for the Richardson plots, rather than the emission current extrapolated to zero field.

A Richardson plot for this sample is shown in Fig. 14.

The work function determined from the slope of this plot is 3.32 volts, and the "A" value is 0.3 amp/cm² degree². A temperature dependence of the work function $d\bar{\Phi}/dT$ will give an apparent work function $\bar{\Phi}'$ of

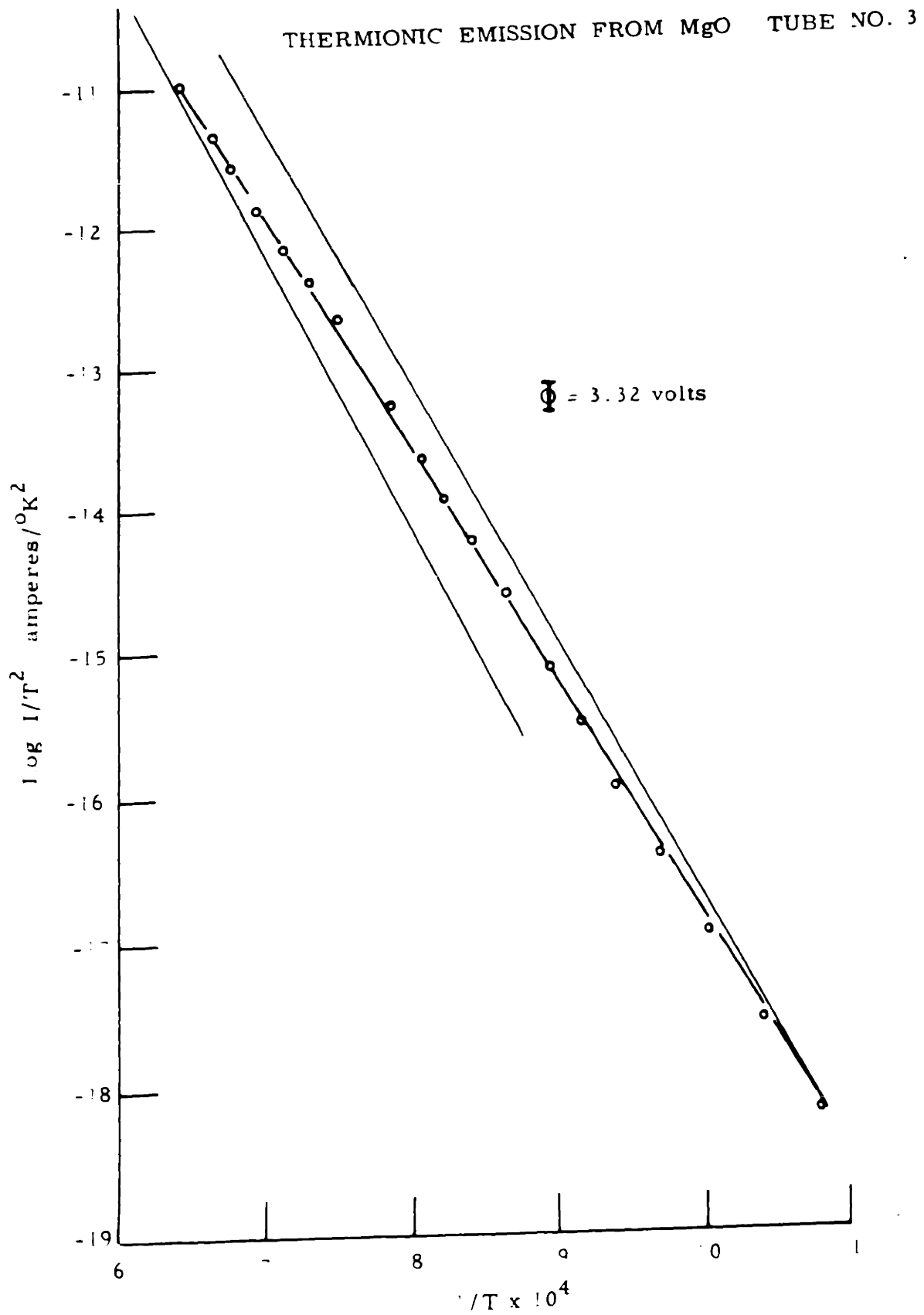
$$\bar{\Phi}' = \bar{\Phi} - T d\bar{\Phi}/dT$$

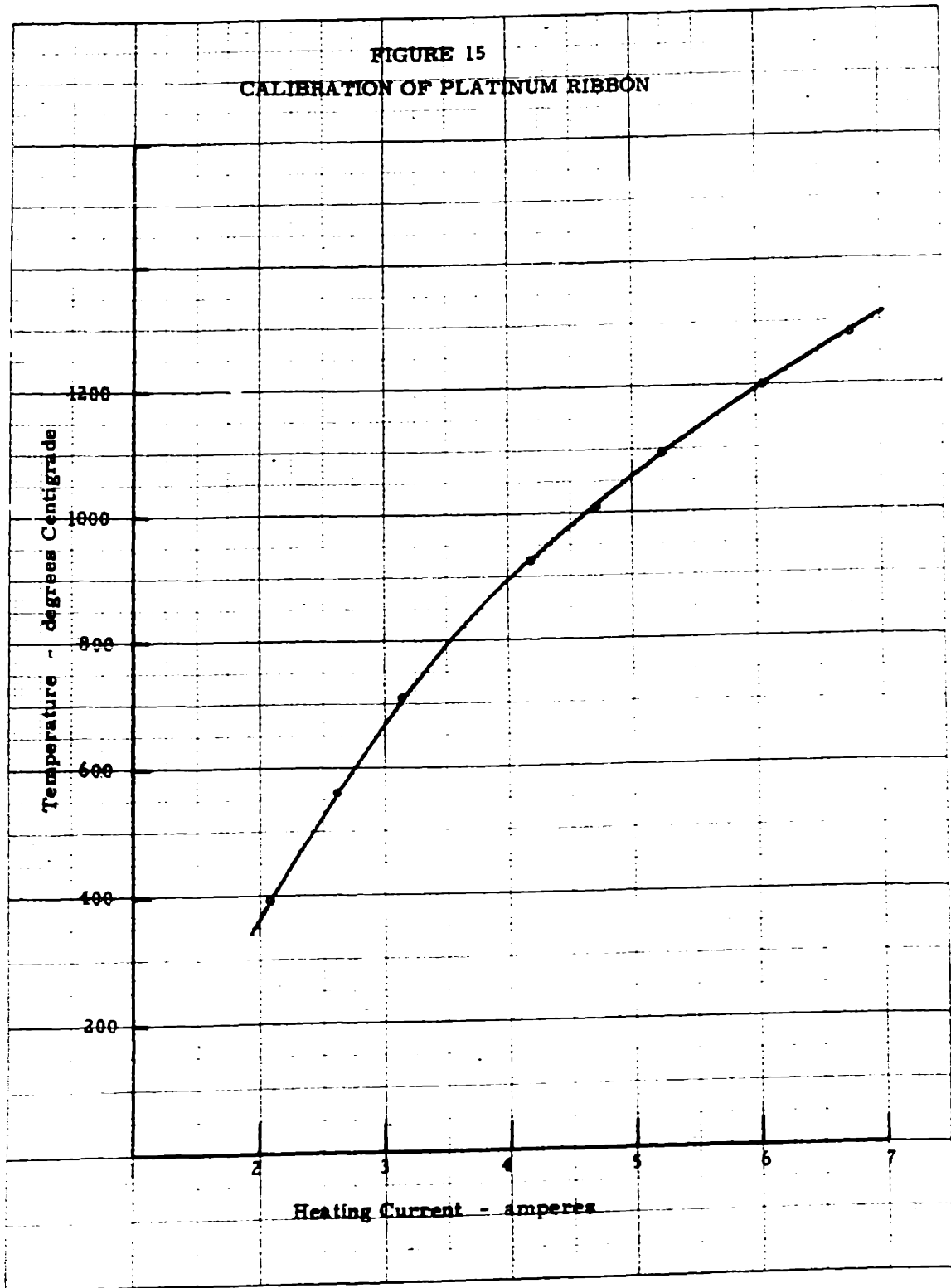
Since a temperature dependence of the work function is indicated by the photoelectric data the value determined from the slope of the Richardson plot is probably lower than the true value. For this reason, the thermionic work function determined by assuming the "A" value to be 120 amp/cm² degree² may be more significant for comparison with the photoelectric thresholds than the more apparent work function. These values, corresponding to the slopes of the light lines in Fig. 14 are 3.6 volts at 900°K and 3.86 volts at 1550°K.

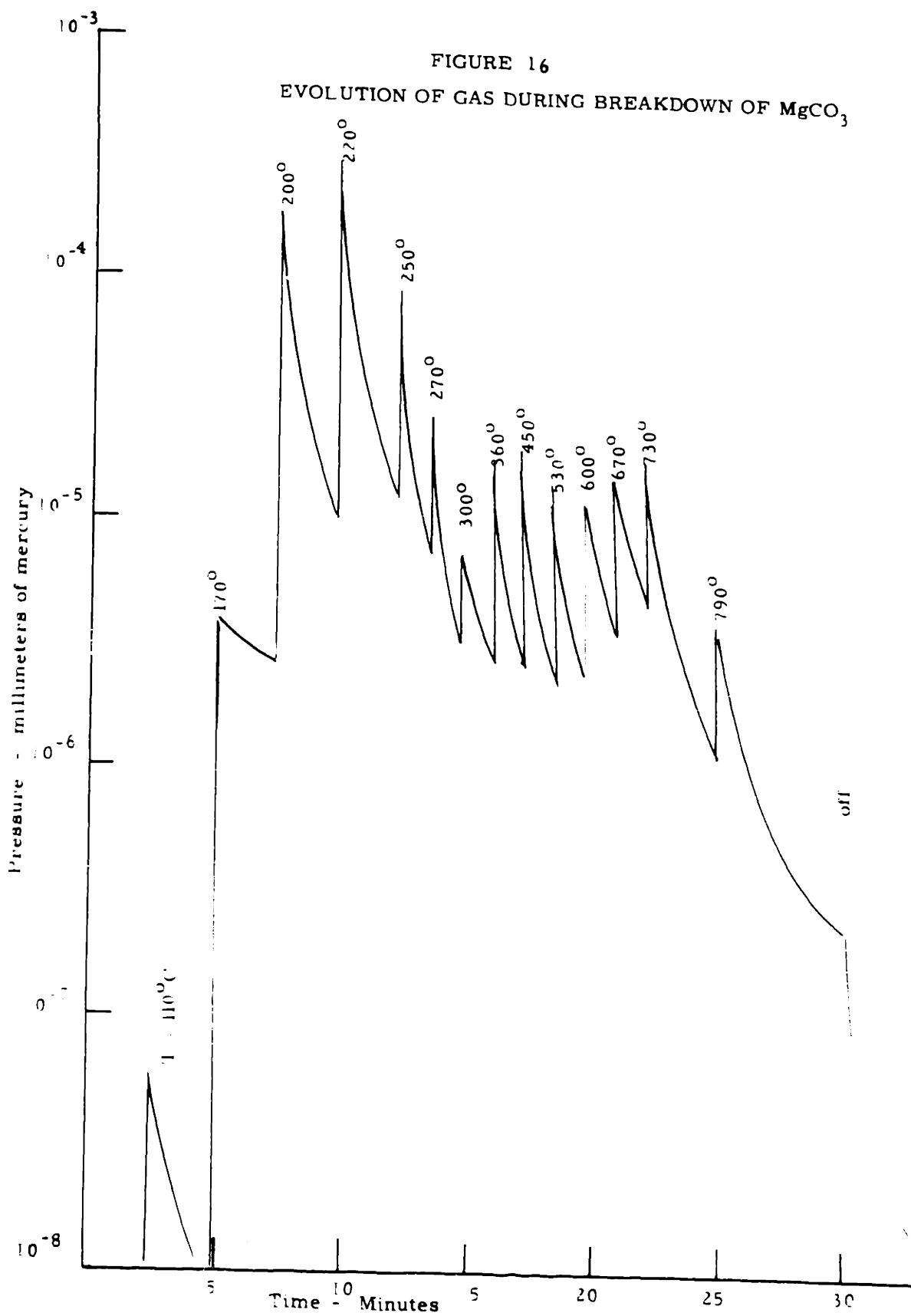
Tube No. 4 was constructed using the platinum ribbon from Tube No. 3 which had been calibrated (Fig. 15) so that the temperature of the ribbon could be determined from the heating current. This allowed thermionic as well as photoelectric measurements to be made on the sample.

During breakdown of the carbonate, the pressure in the tube was recorded as a function of time and temperature of the ribbon. (Fig. 16) These data indicate that the conversion begins at a temperature of 200°C, and is not complete up to the final temperature used for this initial breakdown (790°C).

FIGURE 14







As for Tube No. 2, the photoemission increased as the sample was annealed to higher temperatures. These data are shown in Fig. 17. Curve I is the photoemission after annealing at 790°C . Curve II was taken after the sample had been annealed at 1250°C for one hour. Since the lower peak in the yield curve did not yet appear, the sample was held at 1400°C for ten hours. After this treatment, the photoemission was nearly the same as for Tube No. 2 after annealing to 1400°C , except that the decay of the lower energy peaks in the yield curve was more rapid. For this reason the yield curve was taken at several intervals after flashing the filament. These data are shown in Fig. 18. The curves for 20 seconds and 100 seconds were taken flashing the filament to 1400°C between measurements, but this was not done for long delay times. The decay in the yield curve at high photon energies after an interval of 18 hours is probably due to gas contamination of the surface.

Figure 19 shows the photoelectric yield at about 800°C in the presence of 5×10^{-13} amperes thermionic current. The emission is higher than at room temperature, but the peak in the yield curve at 3.6 eV is now completely obscured. Above 4.0 eV, the yield curve is the same as that for Tube No. 2.

Figure 20 shows a Richardson plot for this tube. The slope of the curve determines a work function 3.6 volts and an "A" value of 3 amperes/cm² degree². If the Richardson "A" value is assumed to be correct, the work function is determined to be 3.85 volts at

FIGURE 17

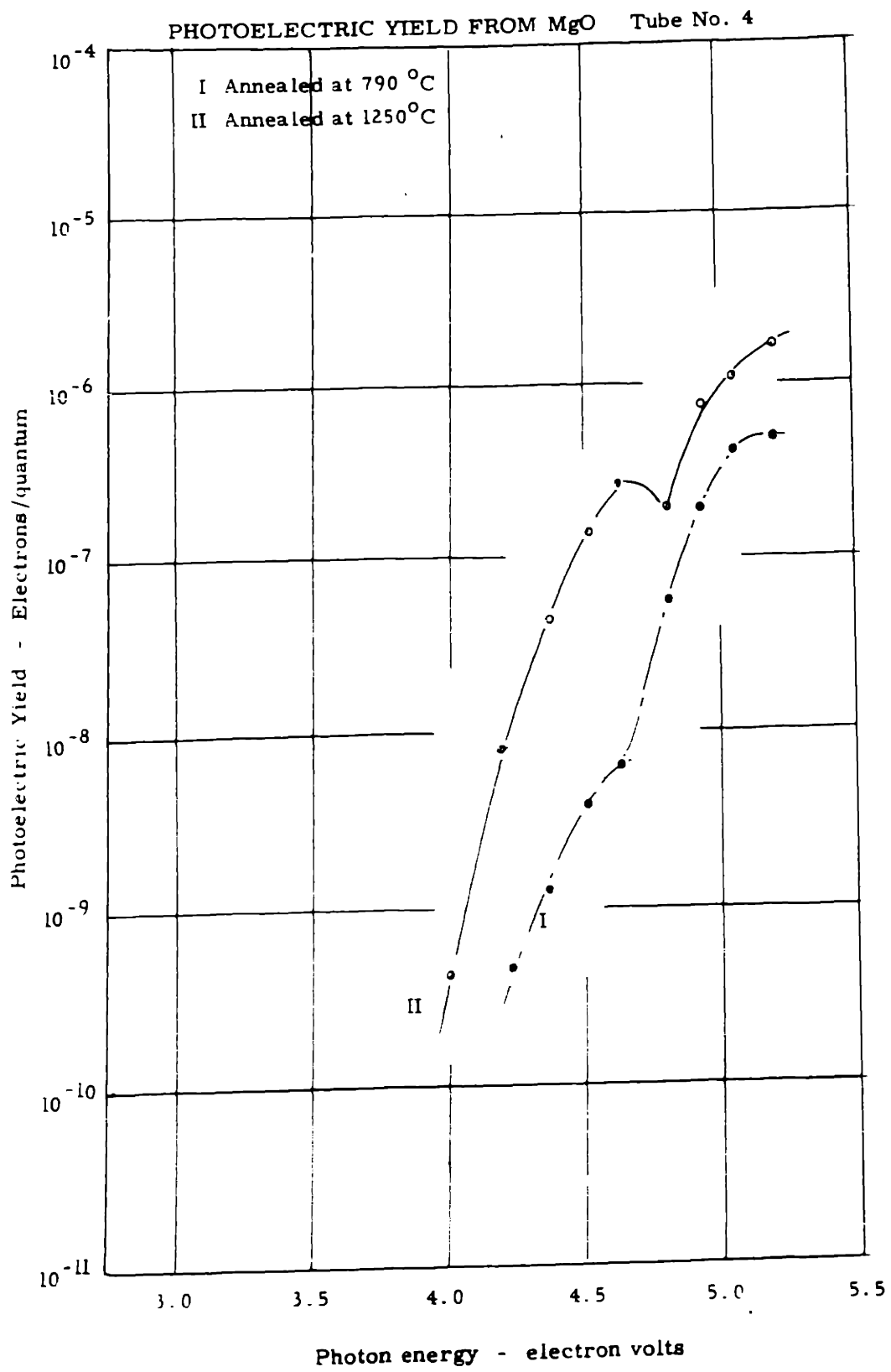


FIGURE 18

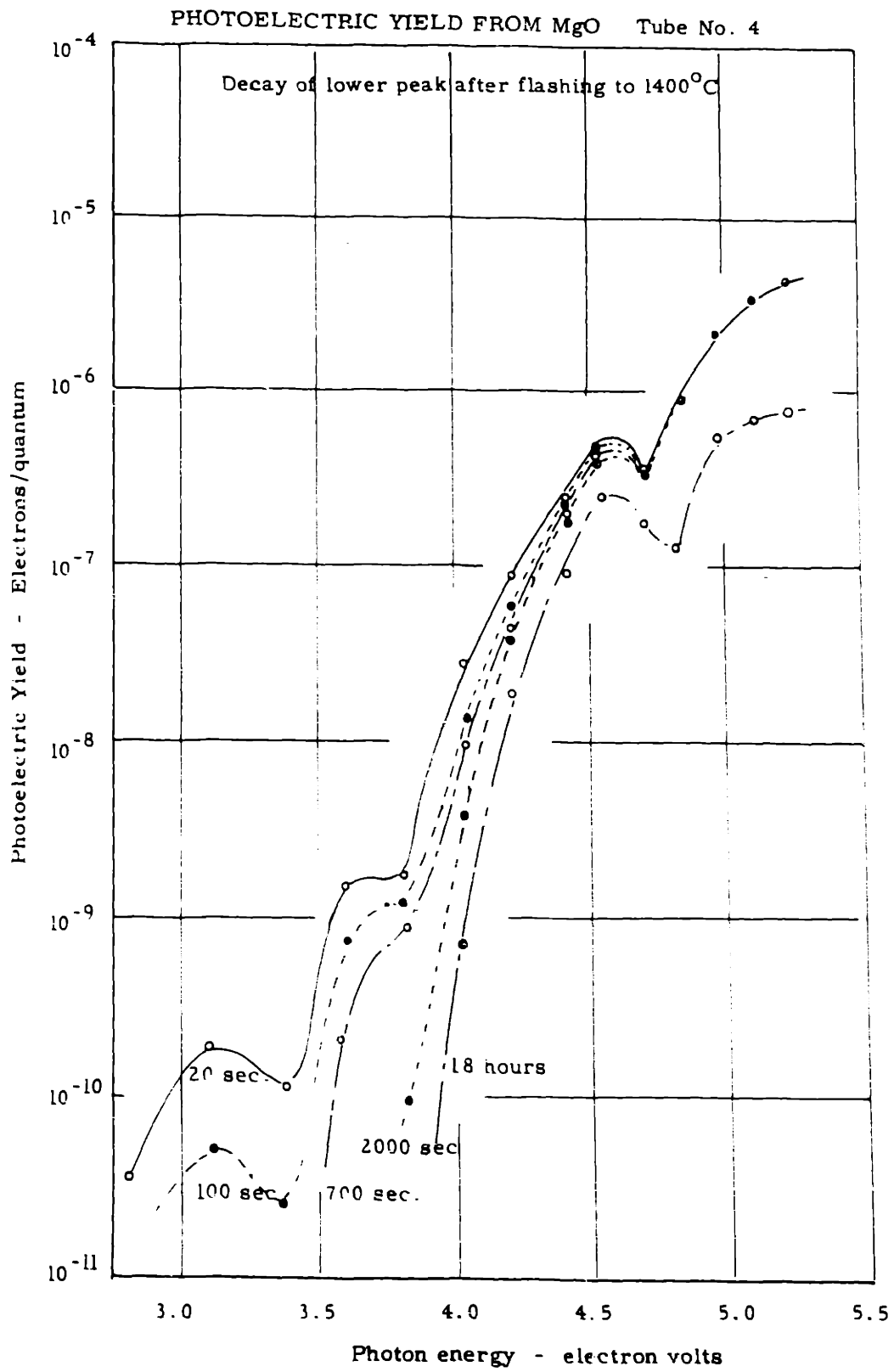


FIGURE 19

PHOTOELECTRIC YIELD FROM MgO Tube No. 4

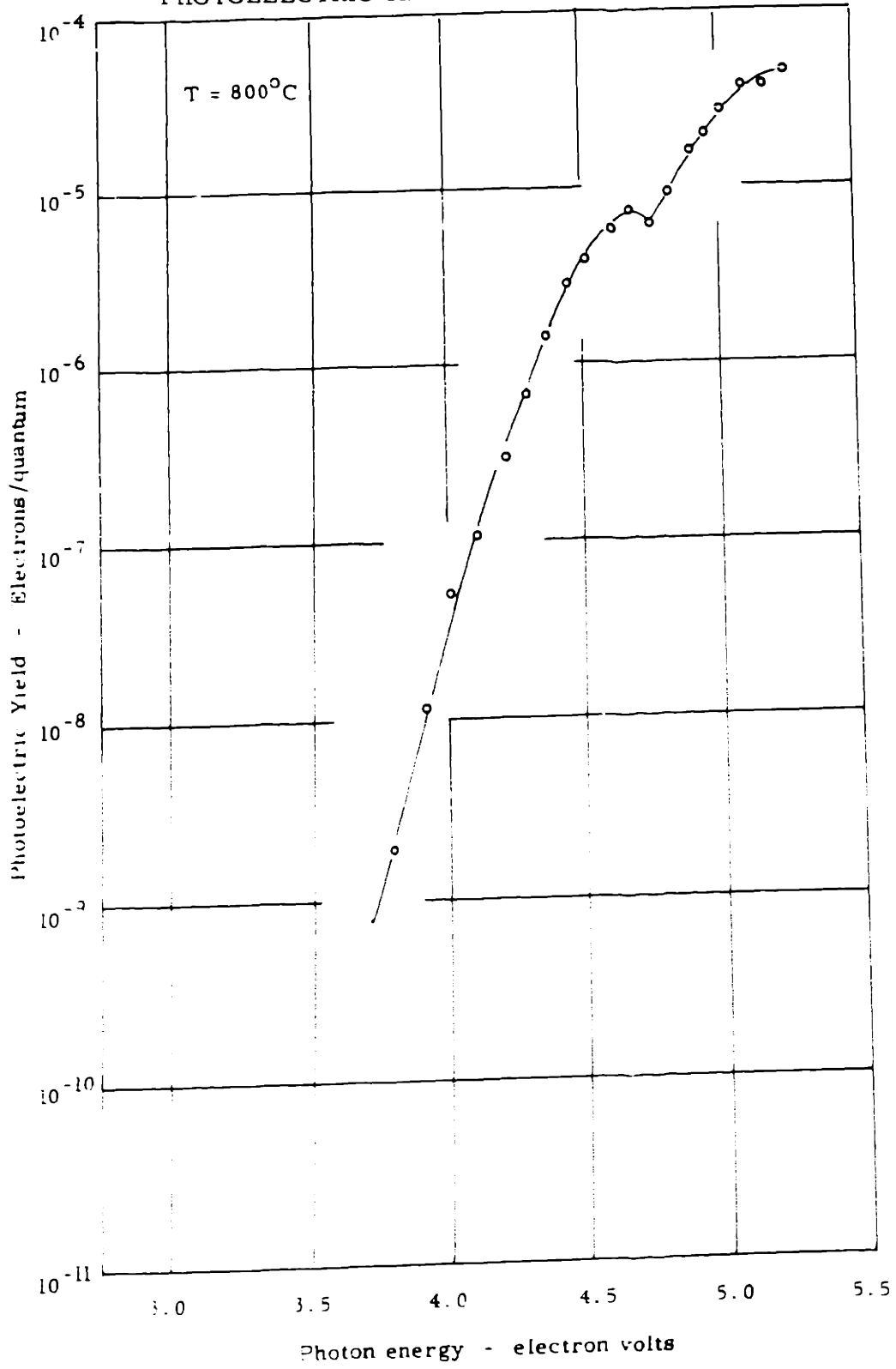
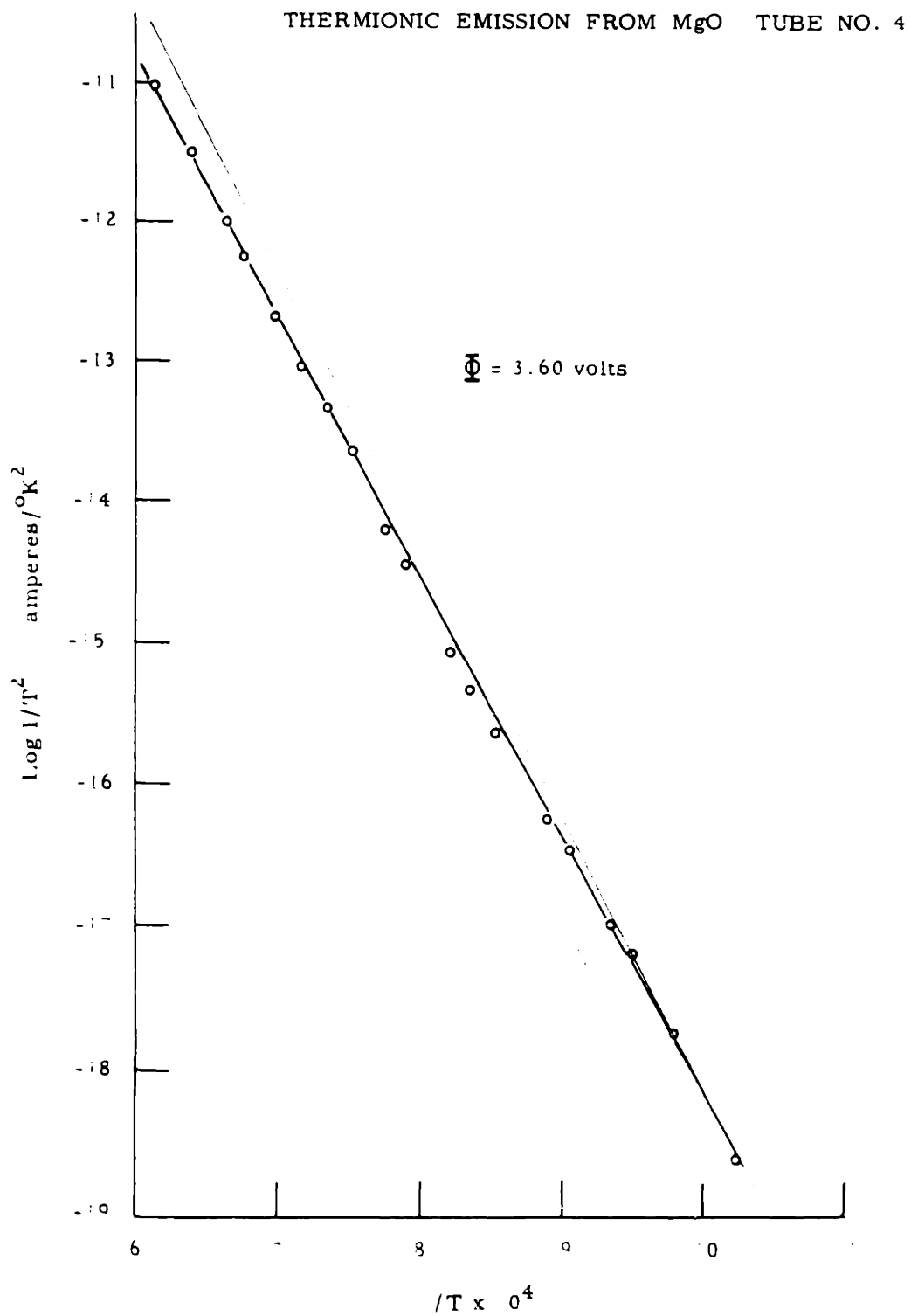


FIGURE 20



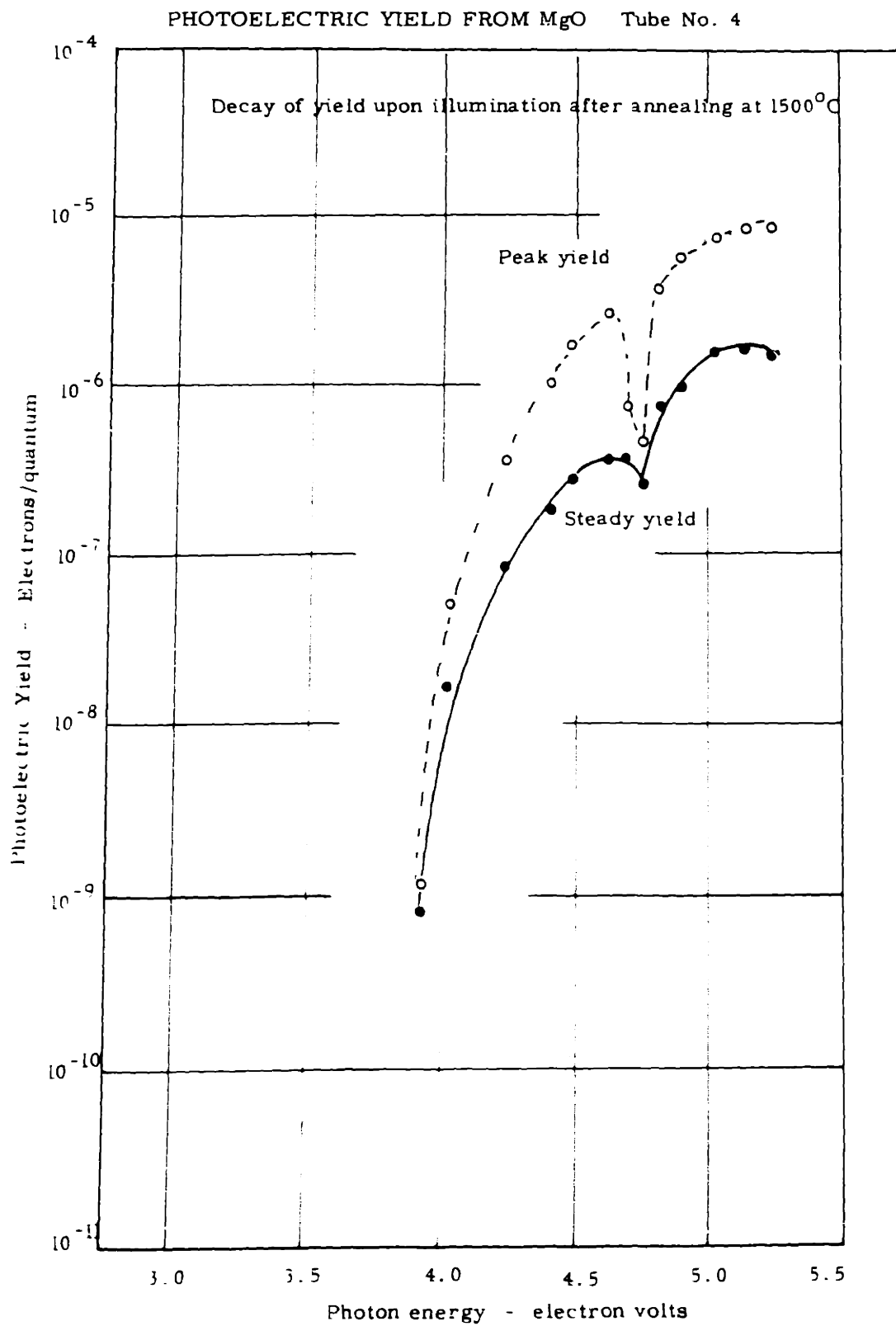
1000°K, and 3.95 volts at 1500°K. These values are somewhat higher than those for Tube No. 3.

In the course of the experiments it was noted that the emission under illumination at 4.0 ev sometimes increased with time, in some cases rising to ten times the initial value and reaching a steady value after 500 seconds. This illumination also enhanced the emission at a photon energy of 3.4 ev, which decayed upon illumination to a value below the limit of detection in some cases, with a similar time constant. Illuminating at 3.4 ev also caused a decay of the emission at 4.0 ev.

Because of the variability of this effect, it is indicated that the impurity levels giving rise to the effect lie close to the Fermi level, and that the occupancy of these levels may change considerably with slight shifts in the Fermi level caused by different processing.

After annealing the cathode in Tube No. 4 to 1500°C, the yield decreased by a factor of 10, and the emission decayed rapidly with illumination, but could be restored by flashing the cathode. Figure 21 shows the peak and steady currents with the cathode held at 800°C. At this temperature the peak value of the current was shown to be restored after waiting for a period of two minutes, so the readings were taken at these intervals. The charge transferred under the pulse was of the order of 10^{-12} amperes, and is not sufficient to explain the decrease in emission due to charging of the surface to the collector potential. Depletion of the centers responsible for the emission seems to be a more likely explanation of this result.

FIGURE 21



D. Summary of Results

The photoelectric yield from magnesium oxide was shown to have a structure with peaks occurring at photon energies of 3.1, 3.6, and 4.6 ev. The photoelectric yield at photon energies below 4 ev was observed after flashing the sample at a high temperature, and was found to decay in time, in some cases more rapidly than others. The yield at low photon energies decreased with temperature at low temperatures but increased with temperature as the thermionic range was approached. Because of the variability of the yield at low photon energies, the photoelectric threshold does not seem to be clearly defined, but depends on the past treatment of the sample. A sample remaining at room temperature for a long time had a threshold of 3.6 ev, although emission was noted at much lower energies after flashing the heater to a high temperature.

Thermionic measurements indicated an apparent work function of 3.3 to 3.6 ev, with corresponding "A" values of .3 and 3 amp/cm² degree².

Enhancement of photoemission at 3.4 ev by radiating at 4.0 ev was found. After annealing the cathode at 1500°C the photoelectric yield was decreased by a factor of ten, and the emission was found to decay upon illumination.

V DISCUSSION OF RESULTS

A. Results on Quartz

The results of the experiments done on quartz in this research are somewhat inconclusive in that the overall sensitivity of the apparatus was not great enough to determine the spectral distribution of the photoemission. The experiments put an upper limit on the photoelectric yield of 10^{-9} electrons per quantum at a photon energy of 4.65 electron volts, and of 10^{-7} electrons per quantum at a photon energy of 5.26 electron volts. Using Apker's ⁽¹⁷⁾ estimate of the absorption cross section for surface states of $2 \times 10^{-17} \text{ cm}^2$, and escape probability of 0.10, this puts an upper limit on the number of surface states lying higher than 4.65 volts below the vacuum level of $5 \times 10^{10} / \text{cm}^2$, and of $5 \times 10^{12} / \text{cm}^2$ at energies above 5.26 volts below the vacuum level. The absorption constant for color centers in alkali halides calculated from this formula ⁽¹¹⁾ is of the proper order of magnitude. It also leads to the correct order of magnitude for quantum yields from metals, assuming only the last atomic layer to be effective in producing photoelectrons. Consequently it is believed to be significant for this calculation.

It was shown that a deposition of a very small amount of tungsten, on the order of .1 monolayer, would change these results drastically, leading to much higher photoelectric yield. The density of the surface states thus introduced was shown to be greater than $10^{13}/\text{cm}^2 \text{ ev}$, indicating that there was probably one surface state introduced for each tungsten atom deposited on the surface. The spectral distribution of the photoelectric yield closely followed the Fowler theory, indicating that the photoemission comes from a distribution of states whose density is constant to a first approximation over the range for which measurements could be made. The work function determined from the Fowler theory was nearly that of metallic tungsten (4.52 ev), and the change of photoelectric yield with gas contaminants on the surface was that expected for tungsten. In spite of this metallic distribution of states, however, the surface resistivity of the sample was greater than 10^{17} ohms per square, as indicated by the fact that the sample would hold a surface charge for several days although the retainer shield in contact with the front surface was held at ground potential. It is interesting to note the magnitude of the quantum yield from this surface compared to that from tungsten. Apker et al ⁽³⁵⁾ have measured the yield from a polycrystalline tungsten surface, and found the quantum yield to be 5×10^{-5} at 5 ev, two orders of magnitude greater than for .1 monolayer of tungsten on quartz.

B. Results on Magnesium Oxide

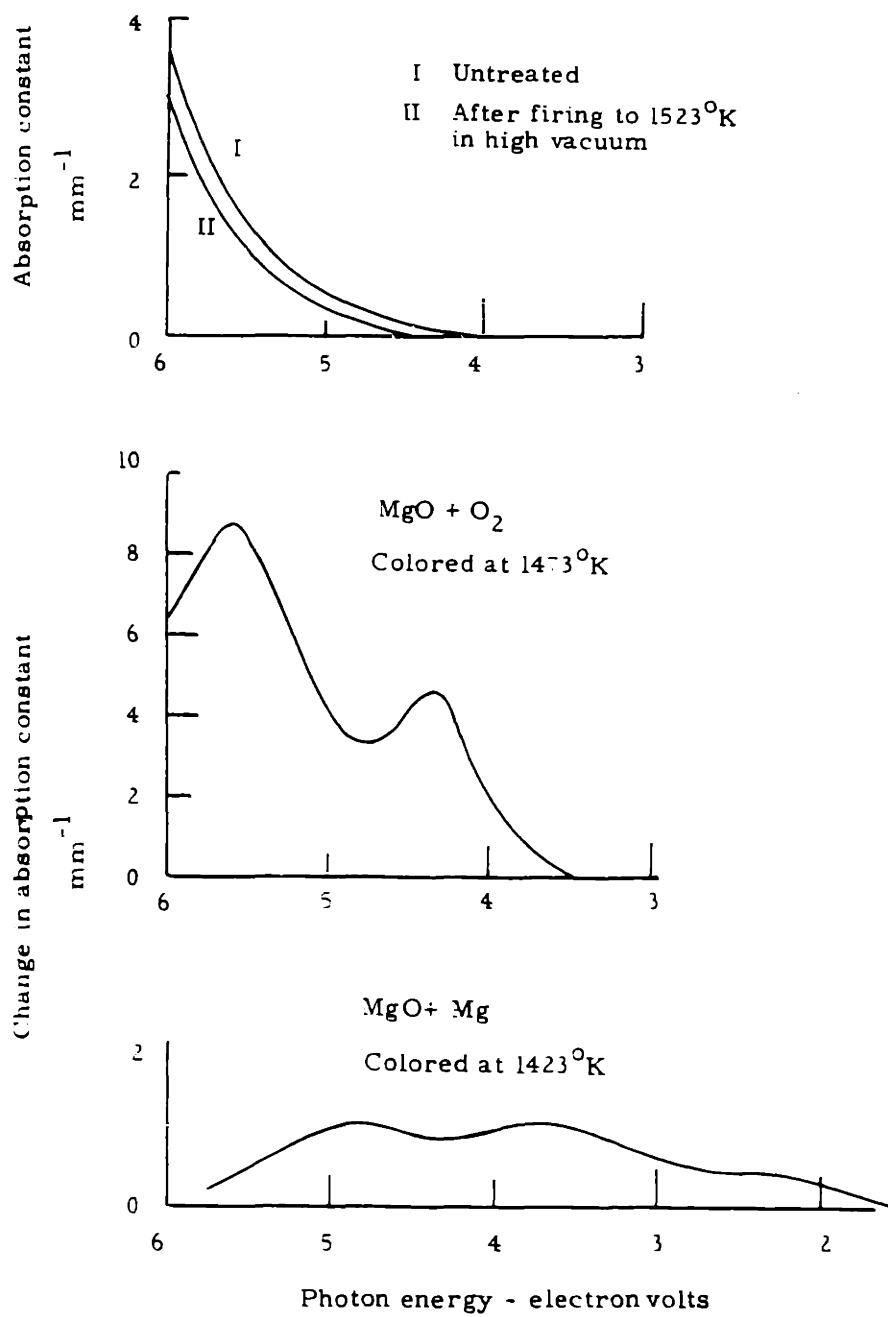
On the hypothesis that the photoemission arises from a continuum of surface states, the yield curve would be expected to be monotonically increasing with photon energy, and show no structure. The yield curve observed for magnesium oxide is inconsistent with such a hypothesis. Consequently a further examination of the electronic structure should be made in an effort to explain the observed results.

The electronic structure of magnesium oxide has not been definitely established, although this material has been studied by a number of investigators. The optical absorption and the absorption induced by heating the crystal in oxygen or magnesium vapor have been measured by Weber ⁽³⁶⁾, and are reproduced in Fig. 21. Similar coloration of magnesium oxide may be introduced by irradiating the crystal with x-rays, ultraviolet light, neutrons, and high energy electrons ^(32, 37, 38). Day ⁽³²⁾ has measured the photoconductivity in crystalline magnesium oxide which had been colored by neutron bombardment, finding peaks at 2.1, 3.7 and 4.8 ev. The identification of the sign of the charge carrier created with absorption of a photon has been made only in the case of the 3.6 band. This was determined to be positive by observing the direction of drift of the region of enhanced photoconductivity at 2.1 ev.

The temperature dependence of the conductivity has been measured by Rochow ⁽³⁹⁾, Lempici ⁽⁴⁰⁾, John ⁽⁴¹⁾ and Mansfield ⁽⁴²⁾.

FIGURE 22

COLORATION OF MgO AFTER H. WEBER



Rochow found the activation energy for conduction in single crystal magnesium oxide to be 1.2 ev over the temperature range of 800° to 1700° K. Lempici found this activation energy for single crystals to be variable below 800° K ranging from .15 to .25 ev. Above 1000° K, the activation energy was found to be 2.2 to 2.3 ev. John measured the activation energy of both single crystal and powdered samples. For the single crystal samples he found an activation energy of 3.0 ev over the temperature range of 1125° K to 1510° K. The compressed pills of powdered magnesium oxide showed an activation energy of 3.2 ev over the same temperature range. Mansfield found the conductivity activation energy of compressed pills to be 2 ev. John and Mansfield have also measured the thermoelectric power for compressed pills. Mansfield found the thermoelectric power to be positive, and attributes the thermoelectric power as positive, (the higher temperature electrode being positive) indicating that the conduction is carried by electrons. Since Mansfield does not define a positive thermoelectric power, and there is some confusion in the literature on this point, it cannot be definitely determined whether these results are in disagreement, or whether Mansfield has incorrectly interpreted his result. The writer feels that the latter is more likely.

Thermionic measurements have been made by Stevenson of the apparent work function of single crystals, and a value of 2.9 volts was found. For a cathode surface of pulverized crystals a value of 3.1 volts was found. The values of the apparent thermionic

work function found in this research were 3.3 to 3.6 volts. Since the values of the conductivity activation energy and the thermionic work function represent the energy differences between the bottom of the conduction band and the Fermi level, and between the vacuum level and the Fermi level, the electron affinity of magnesium oxide may be determined as the difference between these energies. Temperature dependence of the Fermi level has the same effect on the conductivity activation energy as determined from the slope of the $\log \sigma$ vs $1/T$ plot as on the apparent work function determined from the Richardson plot, so the difference should represent the electron affinity quite well. The values which have been obtained are seen to be quite variable, and this is presumably due to variable impurity content in the samples used. However, in the literature quoted above, it seems that the purest samples have the lowest conductivity and the highest activation energy. The value of the electron affinity which is implied from the data above is from 0 to 1.8 ev.

If the electron affinity is of the order of 1 ev, it may be that the peaks in the yield curve correspond to lower energy peaks in the absorption curve. The agreement which is obtained in this way is not good, so this is probably not the correct mechanism. Another possibility is the double mechanism of exciting the electrons into the conduction band from impurity centers, and subsequent absorption of enough energy that they can escape the surface barrier.

If the electron affinity of the crystal were small, electrons which are excited into the conduction band from impurities by the incident rad-

iation would be able to escape, leading to photocurrents which were similar in spectral distribution to the optical absorption and the photoconduction bands. This seems to be the case, as is indicated by the similarity between these distributions.

The forbidden band in magnesium oxide is certainly greater than 6.5 ev, since the absorption constant for photons capable of producing band-to-band transitions would be 10^3 to 10^4 times greater than that found by Weber at 6.5 ev. Since positive carriers are created at 3.6 ev, vacant levels must lie at this energy above the valence band. The results of this research imply that there are filled levels 3.6 ev below the vacuum level. Since the electron affinity is small, it is implied that the forbidden band is not greater than 7.2 ev. In this case, the photoconduction which Day found at 1.2 and 2.1 ev (which were enhanced by ultraviolet radiation) may correspond to the absorption peaks at 4.4 and 5.7 ev found by Weber, indicating a forbidden band width of 6.9 ev. This would agree with the assumption that the absorption bands due to excess magnesium at 2.3 and 4.8 ev were due to the same level, being transitions to that level from the valence band, or from that level to the conduction band.

The proposed energy structure is then a forbidden band of 6.9 ev with levels introduced by excess oxygen at 4.3 and 5.7 ev below the conduction band, and levels introduced by excess magnesium at 2.3 and 3.6 ev below the conduction band.

C. Photoemission for Study of Surface States

In this work there has been no evidence found indicating photoemission from surface states. This implies either that the surface states do not exist on clean surfaces to the degree that has been proposed, or that the estimate of the absorption coefficient and escape probability which has been made is in serious error. It seems to the writer that the former is more likely the case.

APPENDIX

DETERMINATION OF SURFACE STATE DENSITY FROM SHIFT
OF THRESHOLD ON CHARGING THE SURFACE

If a charge $\Delta\sigma$ is deposited on the surface of an insulator, the electronic levels at the surface must be filled to a higher energy to accommodate these extra electrons. The energy difference $\Delta\epsilon$ between the highest occupied levels in the charged and uncharged states will be given by:

$$\Delta\epsilon = \frac{\Delta\sigma}{n(\epsilon)}$$

where $n(\epsilon)$ is the energy density of surface states per unit area at the Fermi level. If the field configuration outside the surface is maintained constant, this change of the Fermi level (or quasi Fermi level since this is not an equilibrium situation) will represent a change in the threshold for photoelectric emission from surface states.

In the case of the quartz samples used, the surface could be charged to 500 volts, and the capacitance across the crystal was ca. $20 \mu\text{pf}/\text{cm}^2$. Thus a surface charge of 10^{-8} coulombs/ cm^2 or 6×10^{10} electrons/ cm^2 is deposited. Since a change in the threshold for photoemission of .01 ev can be observed, a shift will be detected for surface state densities less than $6 \times 10^{12}/\text{ev}\text{-cm}^2$.

This discussion has assumed a uniform density of surface states over the range where the Fermi distribution function differs appreciably from 0 or 1, i. e. assuming that the surface states are spread in energy over a range large compared to kT . In previous

discussions of surface states, some authors have assumed a single energy for these states, largely as a matter of convenience for calculation. If this is actually the case the total density of surface states could be much smaller than the densities indicated above, and still be unobservable by this method.

It may be that the surface electrons do not come to an approximation of the Fermi distribution when they are deposited on the surface, but are trapped in higher levels. However, as a result of the experiments on quartz this does not seem to be the case, since the spectral distributions are the same before and after charging.

ACKNOWLEDGEMENT

The author wishes to express his appreciation to Professor Wayne B. Nottingham for suggesting this work, and for his invaluable interest and help during its progress. Thanks are due to Dr. M. A. Gileo for the calibration of the phototube used, to Mr. A. G. Hall for the preparation of the fused quartz samples, and to Messrs. L. W. Ryan and A. J. Velluto for the glassblowing on the experimental tubes. The author has profited from discussions with the members of the physical electronics group, and from the advice and assistance of Mr. L. E. Sprague.

BIBLIOGRAPHY

1. I. Tamm, Physik Zeits. Sojetunion, 1, 733, (1932)
2. R. de L. Kronig and W. G. Penny, Proc. Roy. Soc. A130, 493, (1931)
3. S. Rijanow, Zeits. f. Physik, 89, 806, (1934)
4. A. W. Maue, Zeits. f. Physik, 94, 717, (1935)
5. E. T. Goodwin, Camb. Phil. Soc., Proc., 35, 205, (1939)
6. E. T. Goodwin, Camb. Phil. Soc. Proc., 35, 221, (1939)
7. W. Shockley, Phys. Rev. 56, 317, (1939)
8. J. C. Slater, Phys. Rev. 45, 794, (1934)
9. H. M. James, Phys. Rev., 76, 1602, (1949)
10. W. G. Pollard, Phys. Rev., 56, 324, (1939)
11. N. F. Mott and R. W. Gurney, Electronic Processes in Ionic Crystals, p. 176, Oxford University Press (1948)
12. Torrey and Whitmer, Crystal Rectifiers, p 51ff, McGraw-Hill (1948)
13. W. E. Meyerhof. Phys. Rev., 71, 727, (1949)
14. J. Bardeen, Phys. Rev., 71, 717, (1949)
15. W. H. Brattain, Phys. Rev., 72, 345, (1947)
W. H. Brattain, Semiconducting Materials, p 37, Butterworth Publications, London, (1951)
16. W. H. Brattain and W. Shockley, Phys. Rev., 72, 345, (1947)
17. L. Apker, E. Taft and J Dickey, Phys. Rev., 74, 1462, (1948)
18. H. Frolich and R. A. Sack, Proc. Phys. Soc., 59, 30, (1947)
19. A. L. Hughes and L. A. DuBridge, Photoelectric Phenomena, p 368 ff, McGraw-Hill, (1932)
20. L Apker, E. Taft and J Dickey, Phys. Rev. 84, 508, (1951)
21. H. B. DeVore and J. W. Dowdney, Phys. Rev., 84, 805, (1951)
22. P. E. Carroll and E. A. Coomes, Phys. Rev., 85, 389, (1952)

23. E. Taft and L. Apker, Phys. Rev. 83, 479, (1951)
Phys. Rev. 82, 814, (1951)
Phys. Rev. 81, 698, (1951)
24. M. H. Hebb, Phys. Rev. 81, 702, (1951)
25. J. A. Becker, Phys. Rev. 34, 1323, (1929)
26. R. C. Hughes, Report on Thirteenth Annual M.I.T. Conference on Physical Electronics. (1953)
27. W. A. Baum and L. Dunkleman, J. Opt. Soc. Am. 40, 782, (1950)
28. D. Alpert and R. T. Bayard, Report on Tenth Annual M.I.T. Conference on Physical Electronics. (1950)
29. D. Jeffries, Master's Thesis, M.I.T. (1950)
30. International Critical Tables, P 134, 341. Vol VI
31. R. R. Law, Rev. Sci. Inst. 19, 920, (1948) and references cited there
32. H. R. Day, ONR Contract No. N7 onr-292 T.O.5, University of Missouri, Technical Report No. 13.
33. L. S. Birks, and H. Friedman, J. Appl. Phys. 17, 687, (1946)
34. W. R. Eubank, J. Amer. Ceram. Soc. 34, 225, (1951)
35. L. Apker, E. Taft and J. Dickey, Phys. Rev. 73, 46, (1948)
36. H. Weber, Zeit. f. Physik 130, 392, (1951)
37. J. H. Hibben, Phys. Rev. 51, 530, (1937)
38. J. P. Molnar and C. D. Hartman, Phys Rev. 79, 1015, (1950)
39. E. G. Rochow, J. Appl. Phys. 9, 664, (1938)
40. A. Lempici, Proc. Phys. Soc. 66B, 281, (1953)
41. O. N. R. Contract No. N7 onr-292 T.O.5, University of Missouri, Progress Reports: Dec. 15, 1952, and March 15, 1953.
42. R. Mansfield, Proc. Phys. Soc. 66B, 1612, (1953)

BIOGRAPHICAL NOTE

Robert Norton Noyce was born in Burlington, Iowa on December 12, 1927. He attended elementary schools in Atlantic, Iowa; Decorah, Iowa; Webster City, Iowa and Grinnell, Iowa. He attended Grinnell High School, and was valedictorian of the Class of 1945.

He entered Grinnell College where he was a Youngkers Scholar in September, 1945, and was elected to Phi Beta Kappa in 1948. During 1948 he was employed in actuarial work by the Equitable Life Assurance Society in New York City, but returned to Grinnell College in February, 1949. He was awarded the A.B. degree in mathematics and physics, with honors, in 1949.

He was admitted to the graduate school of the Massachusetts Institute of Technology in September, 1949. During his graduate work, he served as a teaching assistant in physics, and later as a research assistant in the Research Laboratory for Electronics. He held the Shell Fellowship during the academic year 1950-1951 and was elected to Sigma Xi in 1951. He completed the requirements for the degree of Doctor of Philosophy in physics in September, 1953 and requested the award of the degree at that time.